CHAPTER 1

INTRODUCTION

1.1. BACKGROUND

Water Injection is a method where water is injected back to the reservoir. This is to maintain the pressure in the reservoir. Water used for the water injection is treated and they do not have any oxygen in it. They are usually treated on the oil platform itself. However not all of the platforms have the facilities to do so and because of this they will get their supply of water injection from other platforms which have the facilities. Water Injection rate measurement is critical to ensure that the water injected is sufficient enough to prevent the reservoir from collapsing and to push the oil to the producing wells.

1.2. PROBLEM STATEMENT

Turbine meters are usually used to measure the rate of water injection injected into the reservoir. Turbine meter is an intrusive type meter which means there are moving parts and the fluids are moving in them. A turbine meters uses blades to act as a rotor. The fluid will push the blades and make it spin. This will give an angular velocity which will be calculated and converted to the rate of fluid flowing through it. However, the blades in the water injection turbine meters are easily bent due to the high pressure difference during water injection back on line. These bent turbine blades will affect the accuracy of the reading. As described in the background study, the rate of the water injection injected to the reservoir is very important. Turbine meter is also very expensive. Therefore we have to ensure that it can last long and more reliable.

1.2.1 Significance of the Project

Turbine meters are widely used nowadays especially in the oil and gas industry. With the results from this project, we can create a better and more reliable turbine meters. We can analyze on how stress will be acting on the turbine blade. This will benefit the Oil and Gas company in the long run since the turbine meters will last longer.

1.3. OBJECTIVES AND SCOPE OF STUDY

1.3.1 Objectives

1) To analyse how stress acts on the water injection turbine meter blades

2) To study whether the high pressure difference is the cause of the bent turbine blades.

1.3.2 Scope of Study

The scope of this study would be on stress analysis of water injection turbine meter blade. The initial works are to design the turbine meter blade in CATIA. From there, we can use it to export it to ANSYS for analysis. The operating condition will be simulated in the software. Once the results are obtained, it will be compared with the results from the manual calculations.

The study also focuses on only static analysis since the objective is to study the stress acting towards the turbine blades before it starts to rotate.

The benefits that would be obtained at the end of this research would definitely be helpful to the Oil and Gas Company since a new design could be created to solve the problem of the bent turbine blades.

CHAPTER 2

LITERATURE REVIEW

2.1. STRESS ANALYSIS

Stress analysis is an engineering discipline that determines the stress in materials and structures subjected to static or dynamic forces or loads.

The aim of the analysis is usually to determine whether the element or collection of elements, usually referred to as a structure, can safely withstand the specified forces. This is achieved when the determined stress from the applied force is less than the ultimate tensile strength, ultimate compressive strength or fatigue strength the material is known to be able to withstand, though ordinarily a factor of safety is applied in design.

The factor of safety is a design requirement for the structure based on the uncertainty in loads, material strength, and consequences of failure. Often a separate factor of safety is applied to the yield strength and to the ultimate strength. The factor of safety on yield strength is to prevent detrimental deformations and the factor of safety on ultimate strength is to prevent collapse. The factor of safety is used to calculate a maximum allowable stress.

Factor of Safety is equivalent to the Ultimate Tensile Strength/Maximum allowable stress. When performing stress analysis, a factor of safety is calculated to compare with the required factor of safety. The factor of safety is a design requirement given to the stress analyst. The Analyst calculates the design factor. Margin of safety is another way to express the design factor.

A key part of analysis involves determining the type of loads acting on a structure, including tension, compression, shear, torsion, bending, or combinations of such loads.

Sometimes the term stress analysis is applied to mathematical or computational methods applied to structures that do not yet exist, such as a proposed aerodynamic structure, or to large structures such as a building, a machine, a reactor vessel or a piping system.

A stress analysis can also be made by actually applying the force to an existing element or structure and then determining the resulting stress using sensors, but in this case the process would more properly be known as testing. In this case special equipment, such as a wind tunnel, or various hydraulic mechanisms, or simply weights is used to apply the static or dynamic loading.

When forces are applied, or expected to be applied, repeatedly, nearly all materials will rupture or fail at a lower stress than they would otherwise. The analysis to determine stresses under these cyclic loading conditions is termed fatigue analysis and is most often applied to aerodynamic structural systems.

The evaluation of loads and stresses within structures is directed to finding the load transfer path. Loads will be transferred by physical contact between the various component parts and within structures. The load transfer may be identified visually, or by simple logic for simple structures. For more complex structures, more complex methods such as theoretical solid mechanics or by numerical methods may be required. Numerical methods include direct stiffness method which is also referred to as the finite element method.

The object is to determine the critical stresses in each part, and compare them to the strength of the material. For parts that have broken in service, a forensic engineering or failure analysis is performed to identify weakness, where broken parts are analyzed for the cause or causes of failure. The method seeks to identify the weakest component in the load path. If this is the part which actually failed, then it may corroborate independent evidence of the failure. If not, then another explanation has to be sought, such as a defective part with a lower tensile strength than it should for example.

2.2. TURBINE FLOWMETER

The basic theory behind electronic liquid turbine meters is relatively simple. Fluid flow through the meter impinges upon the turbine blades which are free to rotate about an axis along the center line of the turbine housing. The angular (rotational) velocity of the turbine rotor is directly proportional to the fluid velocity through the turbine. These features make the turbine meter an ideal device for measuring flow rate. The output of the meter is taken by an electrical pickup mounted on the meter body. The output frequency of this electrical pickup is proportional to the flow rate. In addition to its excellent range ability, a major advantage of the turbine meter is that each electrical pulse is also proportional to a small incremental volume of flow. This incremental output is digital in form, and, as such, can be totalized with a maximum error of one pulse regardless of the volume measured. The expanding blade hanger assembly holds the turbine rotor in alignment with the fluid flow. The angle of the blade to the stream governs the angular velocity and the output frequency of the meter. A sharper blade angle provides a higher frequency output. In general, the blade angle is held between 20º and 40º to the flow. Lower angles cause too low an angular velocity and loss of repeatability, while larger angles cause excessive end thrust. The diagram of airfoil can be seen in Figure 2.4 below.

Figure 2.2 is a cross section of the internals of a Turbine Meter. The liquid flows through the turbine meter from left to right. The forward and rear suspension act as flow guides so that fluid motion through the meter is parallel to the meter centerline. Flow impinging upon the angular blades causes the rotor to spin at an angular velocity proportional to flow rate.
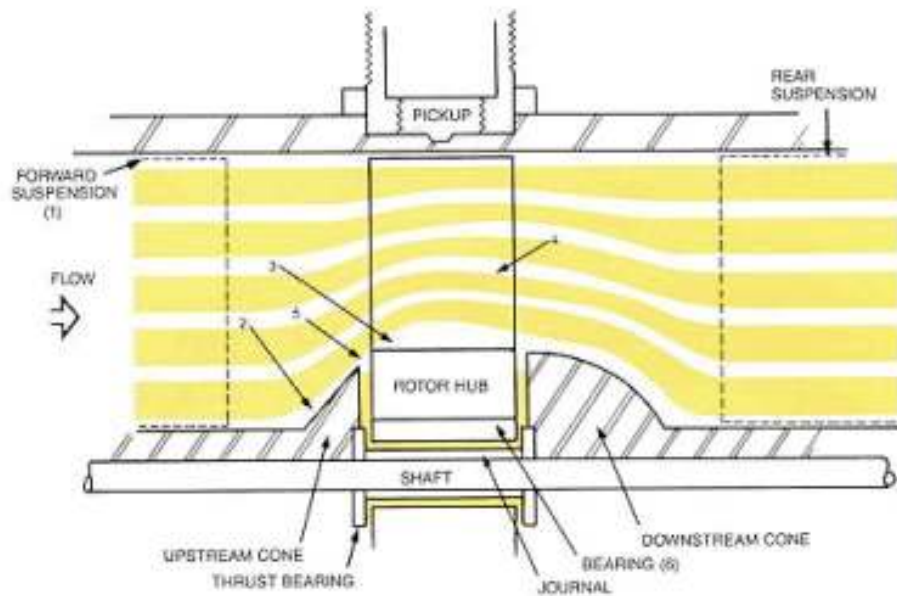
Figure 2.1 Turbine Meter Blades

Figure 2.2: Cross section of the internals of a Turbine Meter

Flowing fluid enters the turbine through the forward suspension, (1). When it encounters the sharp angle of the cone at (2), the stream is deflected outward, increasing in velocity and causing a slight static pressure drop at (3). As the fluid leaves the blade area, flow has redistributed as shown at (4). Velocity is reduced slightly and the static pressure has increased proportionally. The difference between the two velocity pressures causes the rotor to move upstream into the fluid flow. This upstream force would be great enough to cause the rotor to strike the forward thrust bearing,

There are two techniques for analyzing axial turbine performance. The first describes the fluid driving torque in terms of momentum exchange; the second describes it in terms of aerodynamic lift via airfoil theory. The advantage of the former technique is that it readily produces analytical results describing basic operation, some of which have not appeared via airfoil analysis. Although the latter approach allows more complete descriptions using fewer approximations, it is mathematically intensive and leads rapidly into computer-generated solutions. One prominent pioneer of the momentum approach had invented one of the few currently successful dual-rotor turbine flowmeters. There are also turbine meters that are based on the airfoil technique, taking into account, for instance, the effects of blade interference. The following discussion uses the momentum exchange approach as a way to highlight the basic concepts of the axial turbine flowmeter.

In a hypothetical situation, where there are no forces acting to slow down the rotor, it will rotate at a speed that exactly maintains the fluid flow velocity vector at the blade surfaces.
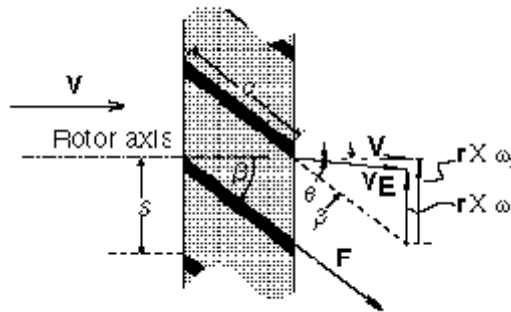

Figure 2.3 Vector diagram for a flat-bladed axial turbine rotor.

The difference between the ideal (subscript i) and actual tangential velocity vectors is the rotor slip velocity and is caused by the net effect of the rotor retarding torques. This gives rise to linearity errors and creates swirl in the exit flow. V incident fluid velocity vector; VE exit fluid velocity vector; θ exit flow swirl angle due to rotor retarding

7

torques; β blade pitch angle, same as angle of attack for parallel flow; ω rotor angular velocity vector; r rotor radius vector; F flow induced drag force acting on each blade surface; c blade chord; s blade spacing along the hub; c/s rotor solidity factor.

Figure 2.3 is a vector diagram for a flat bladed rotor with a blade pitch angle equal to β. Assuming that the rotor blades are flat and that the velocity is everywhere uniform and parallel to the rotor axis, then referring to figure 2.2:

$$r\omega_i = V \cdot \tan\beta \qquad (1)$$

When one introduces the total flow rate this becomes:

$$\frac{\omega_i}{Q} = \frac{\tan\beta}{\bar{r}A} \qquad (2)$$

where ω_i is the 'ideal' rotational speed, Q is the volumetric flow rate, A is the area of the annular flow cross section and $\bar{r}$ is now the root-mean-square of the inner and outer blade radii, (R, a).

Eliminating the time dimension from the left-hand side quantity reduces it to the number of rotor rotations per unit fluid volume, which is essentially the flowmeter K factor specified by most manufacturers. Hence, according to Equation (2), in the ideal situation the meter response is perfectly linear and determined only by geometry. (In some flowmeter designs, the rotor blades are helically twisted to improve efficiency. This is especially true of blades with large radius ratios, R/a. If the flow velocity profile is assumed to be flat, then the blade angle in this case may be described by tanb = constant 3 r. This is sometimes called the "ideal" helical blade.) In practice, there is instead a number of rotor retarding torques of varying relative magnitudes. Under steady flow, the rotor assumes a speed that satisfies the following equilibrium:

8

Fluid driving torque = rotor blade surfaces fluid drag torque + rotor hub and tip clearance fluid drag torque + rotation sensor drag torque + bearing friction retarding torque (3).

Referring again to figure 2.3, the difference between the actual rotor speed, $r\omega$, and the ideal rotor speed, $r\omega_i$, is the rotor slip velocity due to the combined effect of all the rotor retarding torques as described in Eq. (3), and as a result of which the fluid velocity vector is deflected through an exit or swirl angle, θ .. In most flowmeter designs, especially for liquids, the latter three of the four retarding torques described in Eq. (3) are small under normal operating conditions compared with the torque due to induced drag across the blade surfaces. As shown in figure 2.2, the force, **F**, due to this effect acts in a direction along the blade surface and has a magnitude given by:

$$F = \frac{\rho V^2}{2} . C_D . S \qquad (4)$$

where C_D is the drag coefficient and S is the blade surface area per side. Using the expression for drag coefficient corresponding to turbulent flow, this force may be estimated by:

$$F = \rho V^2 0.074 \, Re^{-0.2} . S \qquad (5)$$

where Re is the flow Reynolds number based on the blade chord shown as dimension c in   Figure 2.2.
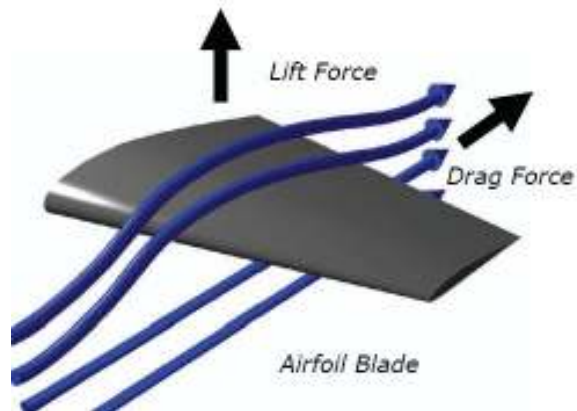
2.3. BLADES

Figure 2.4: Airfoil

Turbine blades usually have an airfoil design. There are two major forces acting on turbine blades as they rotate which are lift and drag. Lift and drag are in constant competition, acting to cancel each other out. With higher pressure on the flat side of the blade and lower pressure on curved side, lift is created. The blade is pulled toward the area of low pressure in the direction of the lift force. This will make the blade rotates.
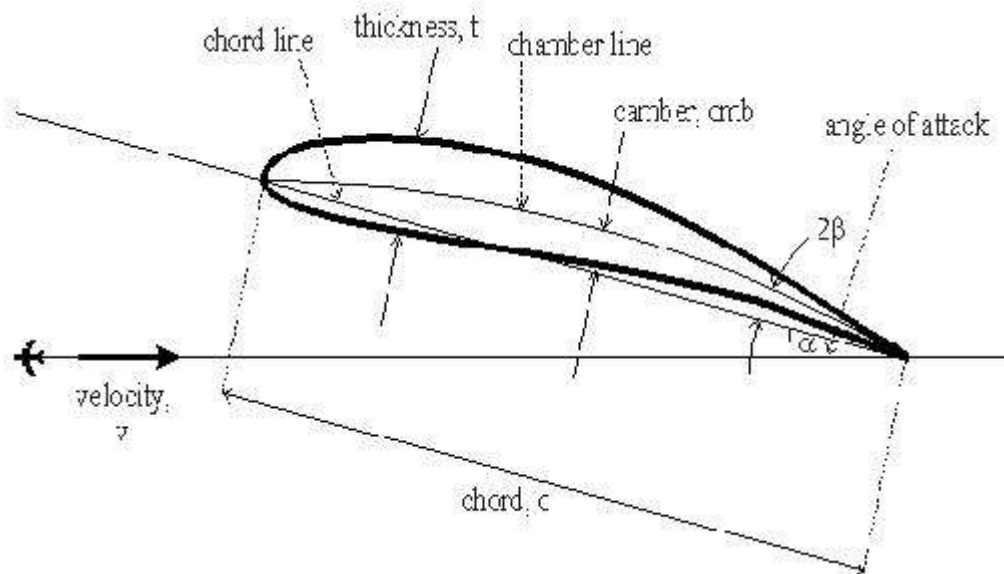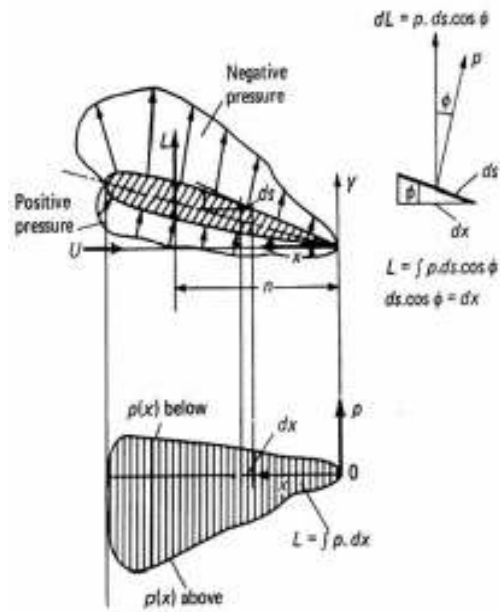

Figure 2.5: Diagram of Airfoil

Figure 2.6 Pressure Distribution of an Airfoil

Figure 2.6 shows the pressure distribution of an Airfoil. This is as assumption of distribution of pressure on the turbine blades since it is using an airfoil design. In the figure, it is shown that the pressure below which is acting on the airfoil is higher compared to the pressure which is situated above the airfoil. This proves that the statement above is true and lift will be created. The lift force can be represented by:

$$L = C_L \times \rho \times \frac{V^2}{2} \times A \quad (6)$$

2.4 TRANSIENT STATE STRESS ANALYSIS ON AN AXIAL FLOW GAS TURBINE BLADES AND DISK USING FINITE ELEMENT PROCEDURE

According to Sukhvinder Kaur Bhatti, Shyamala Kumari, M L Neelapu, C Kedarinath and Dr. I N Niranjan Kumar, they had done a stress analysis on an axial flow gas turbine blades and disk using finite element procedure. The objective of the study is to provide understanding and information for designers to improve the life and efficiency of future generations of engines. The analysis of stress values that are produced while the turbine is running are the key factors of study while designing the next generation gas turbines. A gas turbine rotating system is loaded with time by the changes in stress levels as a result of start-up and shutdown procedures. Hot section blades typically fail because of creep, oxidation, low-cycle fatigue (LCF), and high-cycle fatigue (HCF). Contributing factors often include environmental attack, corrosion, cyclic loads, over firing, or inadequate refurbishment. Hot section blading are life-limited items and require refurbishment or replacement at intervals dependent upon thermal exposure. The "heart" of these versatile machines is made by the blades and vanes, which are subjected during operation to very high thermal and mechanical stresses (combined effects of centrifugal force and thermal gradient), in aggressive environment. The research on gas turbine cooling systems is coupled with the flow and heat transfer associated with rotating turbine. Therefore this report has primarily focused on the Transient heat transfer characteristics, centrifugal and the thermal stresses arising in the disk. The maximum stresses obtained from different analysis by using innovative high heat resistant material INCONEL 718 are found to be within the yield strength of the material. ANSYS was used to do a Hoop, Radial and Vonmises Stress and Thermal Analysis. Maximum operational radial stress which is a combination of thermal and structural analysis is obtained as 800 MPa. The maximum operational hoop stress is 802 MPa and finally the maximum operational Vonmises stress is 878 MPa. All the above values are within the yield strength of the material. From the results, the disk is expected to perform well in spite of all the stringent operating conditions.

2.5. MATERIAL OF THE TURBINE BLADE

The rotor blade design was based on the Brooks Parity turbine flowmeter from Fisher-Rosemount Petroleum. The turbine meter is a 12 inch model. Before designing the turbine blades, the material of the turbine blade should be determined. This is because the material needs to be identified before the meshing process can be done. There are many materials that can be used for the Turbine blades such as Aluminum, Stainless Steel and Titanium. However, for this project we will be using 430 Stainless Steel as the material of the Turbine Blade. Table 2.1 shows the material properties of 430 Stainless Steel.

Table 2.1: Material Properties of 430 Stainless Steel

PROPERTIES	VALUE
Grade	430
Tensile Strength (MPa)	450
Proof Stress 0.2%(MPa)	205
Elongation A5 (%)	22
Hardness Rockwell B (HR B)	89 max
Density (g/cm3)	7.75
Melting Point (°C)	1425-1510
Modulus of Elasticity (GPa)	200
Electrical Resistivity (Ω.m)	$0.06X\ 10^{-6}$
Thermal Conductivity (W/m.K at 100°C)	23.9
Thermal Expansion (/K at 100°C)	$10.4\ X\ 10^{-6}$
Yield Strength (MPa)	290-430
Poisson Ratio	0.27-0.30

CHAPTER 3

METHODOLOGY/PROJECT WORK

3.0. METHODOLOGY/ PROJECT WORK

3.1 Project Flow Chart
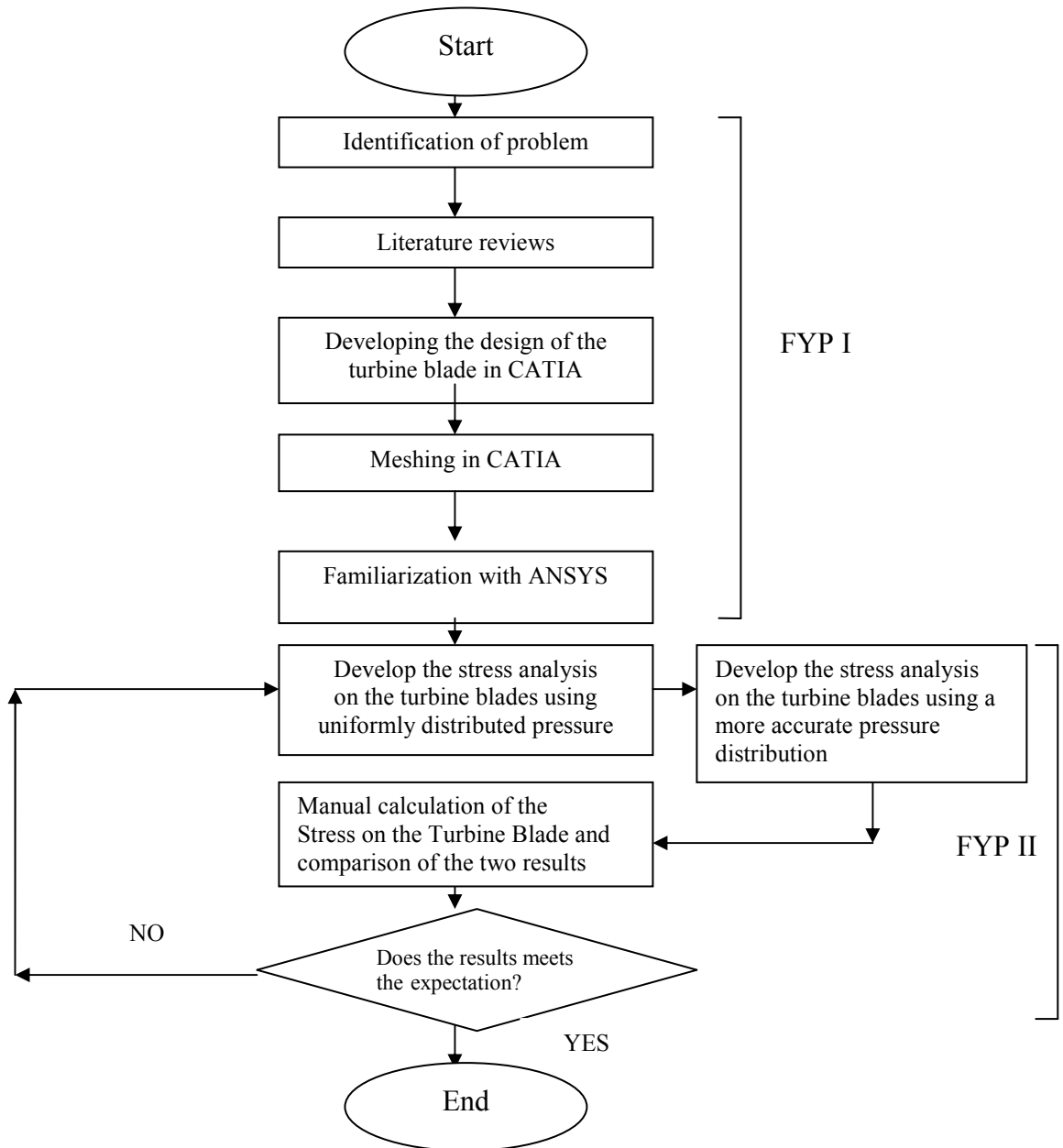
Figure 3.1: Project Flow Chart

3.2 Tools/Equipment Required

The tools and equipment which are required in this Final Year Project are a Windows based PC together with the programs such as Microsoft Office. CATIA will be used for the designing of the turbine blade. After designing the turbine blade, the file will be imported to ANSYS. ANSYS is used to develop the stress analysis on the turbine blades. Other equipment needed basically would be data from on site results as well as from the internet and other references. Microsoft Office programs include Microsoft Word are used to type reports, Microsoft Excel to draw graphs and rearranging of data.

3.3 Developing the Design of the Turbine Blade

In developing the design of the turbine blade, CATIA will be used. CATIA which stands for Computer Aided Three-dimensional Interactive Application is a multi-platform CAD/CAM/CAE commercial software suite. CATIA is widely used throughout the engineering industry, especially in the automotive and aerospace sectors. CATIA was chosen because we can design the turbine blade and import it to ANSYS to do the stress analysis. For the design of the turbine blade, the Brooks Parity turbine flowmeter from Fisher-Rosemount Petroleum was used. It is a volumetric flow measurement and transmitting device used extensively in the petroleum industry. The design will be based on a 12 inch diameter model.

3.4 Collection and Calculations of Data

Before any simulation can be done, the data must be collected and calculated. For the simulation, the data collected and calculated will be discussed in the subtopic 3.6. Those data are important if the simulation stage is to be proceeded.

3.5 Meshing in ANSYS

Previously in FYP I, the meshing of the turbine blades was done in CATIA. However, further studies showed that meshing in ANSYS would be more accurate and it will be easier to do the stress analysis if it is meshed in ANSYS. Before any work is taken place in ANSYS, familiarization of the software was done. This includes in doing some

tutorials which were provided with the software. Meshing can be done in many ways by selecting different elements. The finer the element is, the more accurate the result is. The material properties should also be stated. The main property that is needed is Young's Modulus and Poisson Ratio. Table 2.1 shows the properties of the materials which is the 430 Stainless Steel. Next the element of the material is chosen. In this turbine blade case, the element Solid 10Node187 was chosen to be used for the turbine blade. Figure 3.3 shows the window for choosing the elements of the turbine blades. This element was chosen since it was proposed by the software for a better result. Below is a table of the material properties which are used for the turbine blade material.
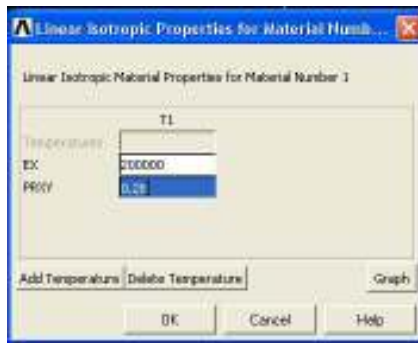
Figure 3.2: Properties   Figure 3.3: Element types
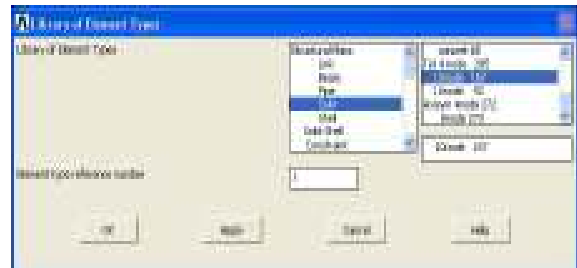
Once this are completed, the size of element must be defined before it can be meshed. For this project the element size is set to be 2mm due to the turbine blade's size. If a bigger size was set, the results of the stress analysis would not be accurate.

Table 3.1: Element size

PROPERTIES	VALUE
Element size (mm)	2

3.6 Developing the stress analysis on the Turbine Blades

The stress analysis of the Turbine Blades will be conducted by using ANSYS. ANSYS is a software that can develop a general-purpose finite element analysis and computational fluid dynamics software. By using ANSYS, results on how the stress affects the turbine blade can be obtained. The types of stress that are acting towards the blades also can be identified through ANSYS. The results will show the most vulnerable part of the turbine blade when there is a high pressure difference that is acting towards the blade. With the result, a better design of the turbine blade could be achieved in the future. To achieve this result, the real operating condition will be simulated in ANSYS. The turbine meter blades are exposed to a high pressure difference. The blades will be exerted a pressure of 8000kpag which is a normal pressure for a water injection pipeline.

For this project, two simulations will be done. One with the pressure distributed uniformly throughout the surface of the airfoil and the other using an approximate of the actual pressure distribution on the turbine blade. For this purpose, the data of NACA 4415 will be used. An assumption was made so that the pressure distribution is the same to reduce complications.

i) Uniformly Distributed Pressure

In ANSYS, the load that will be applied on the airfoil will be pressure. As discussed previously, pressure will be acting on both top and bottom surface of the airfoil with the bottom pressure having the bigger pressure. Figure 3.4 shows how the value of the pressure being applied.
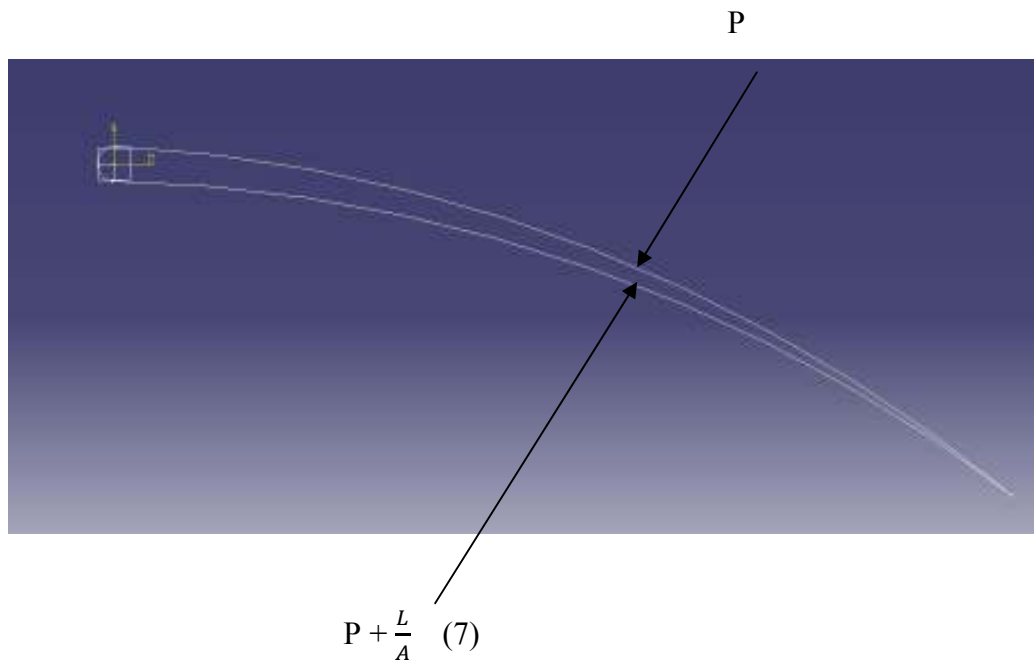
P

$$P + \frac{L}{A} \quad (7)$$

Figure 3.4: Value of the pressure applied on the Turbine Blade

With P = Water Pressure = 8000kPa

L = Lift Force

A = Area = Chord Length X Width

Figure 3.5 shows the NACA 4415 Airfoil Blade and Figure 3.6 shows the pressure coefficient distribution of NACA 4415 Airfoil.
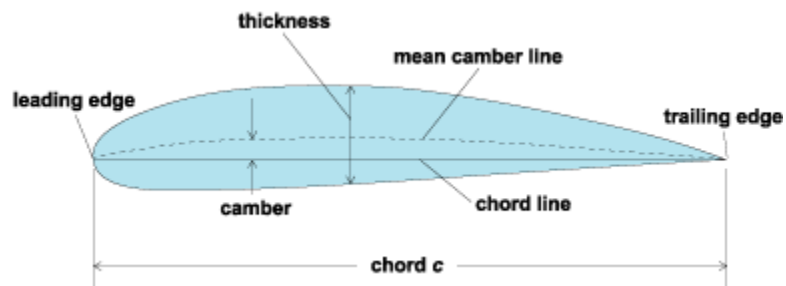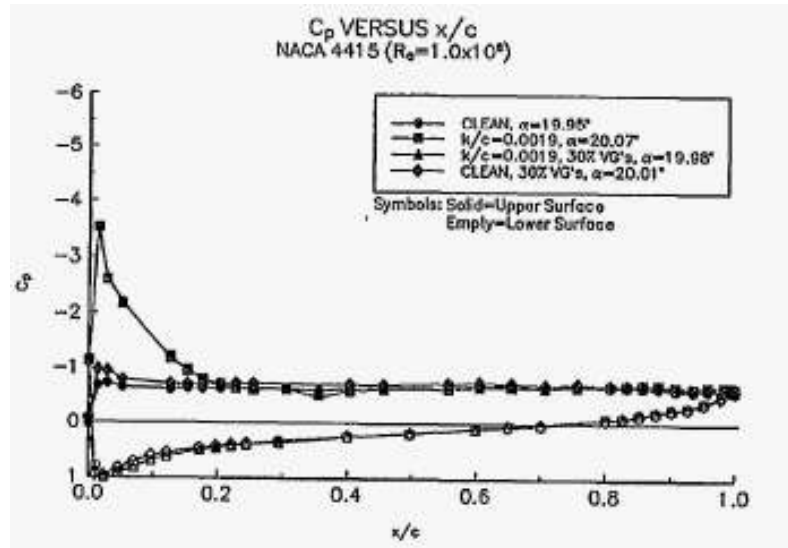

Figure 3.5: NACA 4415 Airfoil Blade

Figure 3.6: NACA 4415 Pressure Coefficient Distribution

With using the data from NACA 4415 the value of $\frac{L}{A}$ can be calculated. Table 3.3 shows the data collected. Even for the uniformly distributed pressure, the data from NACA 4415 is required to calculate the lift force such as the lift coefficient which is used to calculate

Table 3.2: Operating Condition Data collected

	Units
Pressure (kPa)	8000
Width (m)	0.08
Chord Length (m)	0.0894
Lift Coefficient	1.9
Water Density (kg/cubic m)	1025
Velocity (m/s)	5.216

- Lift Force

$$L = \frac{1}{2}\rho v^2 A C_L \qquad (6)$$

L = 0.5 X 1025 X 5.22 X5.22 X 0.0072 X 1.9

L= 189.47N

- Area

A= Chord length X Width $\qquad (8)$

A= 0.0894m X 0.08m

A= 0.0072 m squared

- L/A = 189.47/0.007152

= 26492.48 Pa

= 26.49 kPa

Due to this,

$P_\circ$ = 8000kPa

$P_\circ$ + L/A = 8000 + 26.49 $\qquad (7)$

= 8026.49 kPa

Once the data are calculated, the simulation will be done in ANSYS with the assumption the pressure will be uniformly distributed throughout the bottom and the top surface of the turbine blade.

ii) Actual Pressure Distribution in assumption to NACA 4415

For the second part, the simulation will be done by using the actual pressure distribution in assumption to NACA 4415. With the data from Figure 3.6, the pressure distribution can be calculated and divided into certain sections. In this case, the author had decided to divide the pressure distributions to 10 sections. The 10 sections will be divided in respect to the chord length of the turbine blade which is 89.4mm.

The Coefficient of Pressure is defined as:

$$C_P = \frac{P - P_\infty}{q_\infty} \qquad (9)$$

Where P = Local Static Pressure

P_∞ = Freestream Static Pressure

q_∞ = Freestream Dynamic Pressure ($\frac{PV^2}{2}$)

Since P is to be determined, the equation is rearranged to:

$$P = \left(\frac{1}{2}\rho V^2 C_p\right) + P_\infty \qquad (10)$$

Table 3.3 shows the data for the pressure which is acting towards the top surface of the turbine blade and Figure 3.7 shows the graph of the pressure distribution for the top surface of the blade.

Table 3.3: Data of the pressure acting towards the top surface of the blade

$P_\circ$ (kPa)	Density (kg/m^3)	Velocity (m/s)	Length %	Cp	P (kPa)
8000	1025	5.216	0	-1.2	7983.3
8000	1025	5.216	5	-3.5	7951.2
8000	1025	5.216	10	-1.5	7979.1
8000	1025	5.216	20	-0.9	7987.5
8000	1025	5.216	30	-0.9	7987.5
8000	1025	5.216	40	-0.9	7987.5
8000	1025	5.216	50	-0.9	7987.5
8000	1025	5.216	60	-0.9	7987.5
8000	1025	5.216	70	-0.9	7987.5
8000	1025	5.216	80	-0.9	7987.5
8000	1025	5.216	90	-0.9	7987.5
8000	1025	5.216	100	-0.9	7987.5
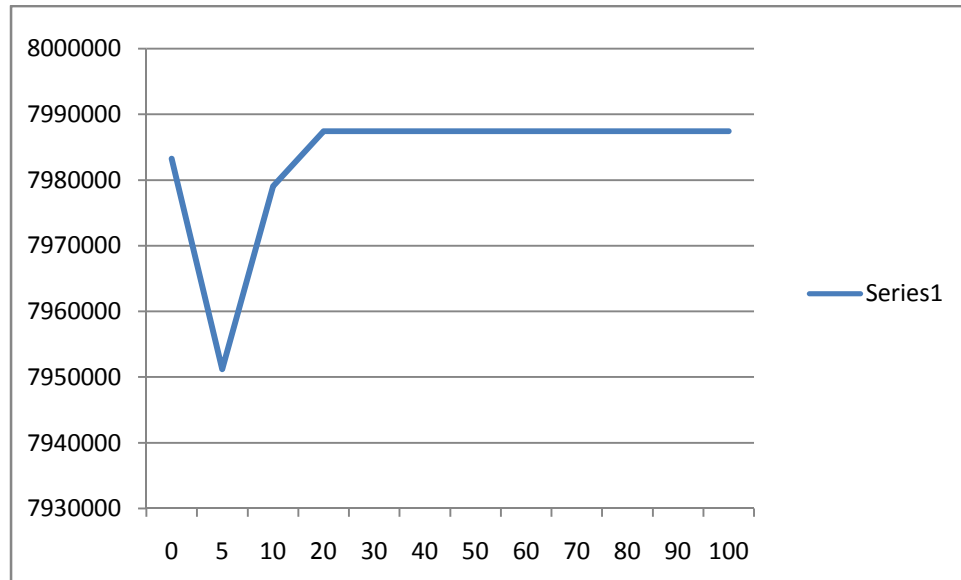
Figure 3.7: Graph of the pressure distribution for the top surface of the blade

Table 3.4 shows the data for the pressure which is acting towards the bottom surface of the turbine blade and Figure 3.8 shows the graph of the pressure distribution for the bottom surface of the blade.

Table 3.4: Data of the pressure acting towards the bottom surface of the blade

$P_\circ$ (Pa)	Density(kg/m^3)	Velocity (m/s)	Length %	Cp	P
8000	1025	5.216	0	1	8013.9
8000	1025	5.216	5	0.8	8011.2
8000	1025	5.216	10	0.6	8008.4
8000	1025	5.216	20	0.4	8005.6
8000	1025	5.216	30	0.3	8004.2
8000	1025	5.216	40	0.2	8002.8
8000	1025	5.216	50	0.1	8001.4
8000	1025	5.216	60	0.05	8000.7
8000	1025	5.216	70	0	8000
8000	1025	5.216	80	-0.1	7998.6
8000	1025	5.216	90	-0.2	7997.2
8000	1025	5.216	100	-0.9	7987.5
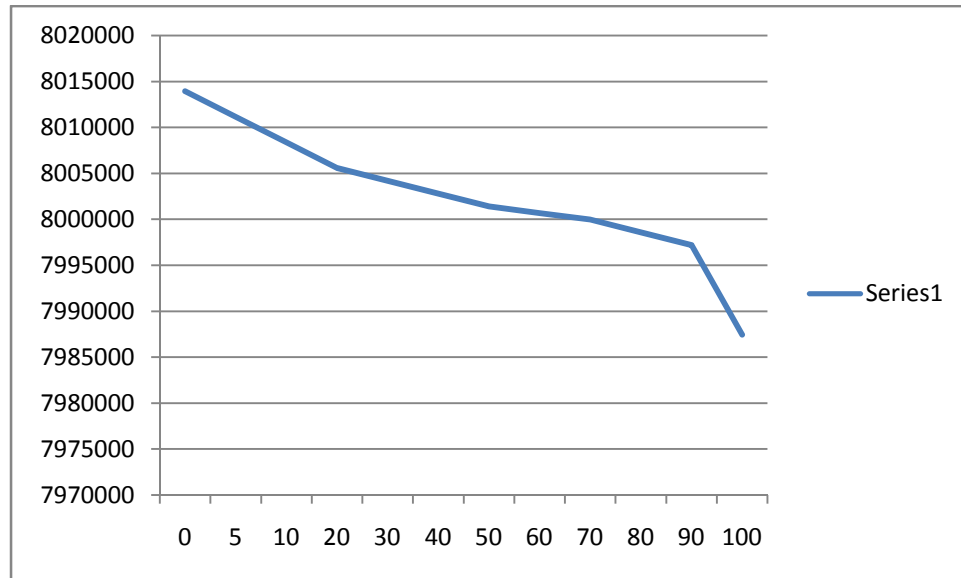
Figure 3.8: Graph of the pressure distribution for the bottom surface of the blade

From these data, the simulation using the assumed pressure distribution can be done.

3.7. Manual calculation and the comparison between the ANSYS and the manual calculation results

Manual calculation on the stress which acts towards the turbine blade is to be measured. This is done so that a comparison of results can be made between the ANSYS simulation and the manual calculation. Comparison is done so that the results produced by the simulation can be verified. It is expected that both results should be quite similar even though there might be slight difference between the two results.

3.8. Gantt Chart

Please refer to the Appendix for Gantt chart for FYP I and FYP II.

CHAPTER 4

RESULTS AND DISCUSSION

4.1. RESULTS

4.1.1 The Design of the Turbine Blade

For the design of the turbine blade, CATIA was used. Two designs are made which are the rotor blade and the single turbine blade. The figures below show the designs of the blade.
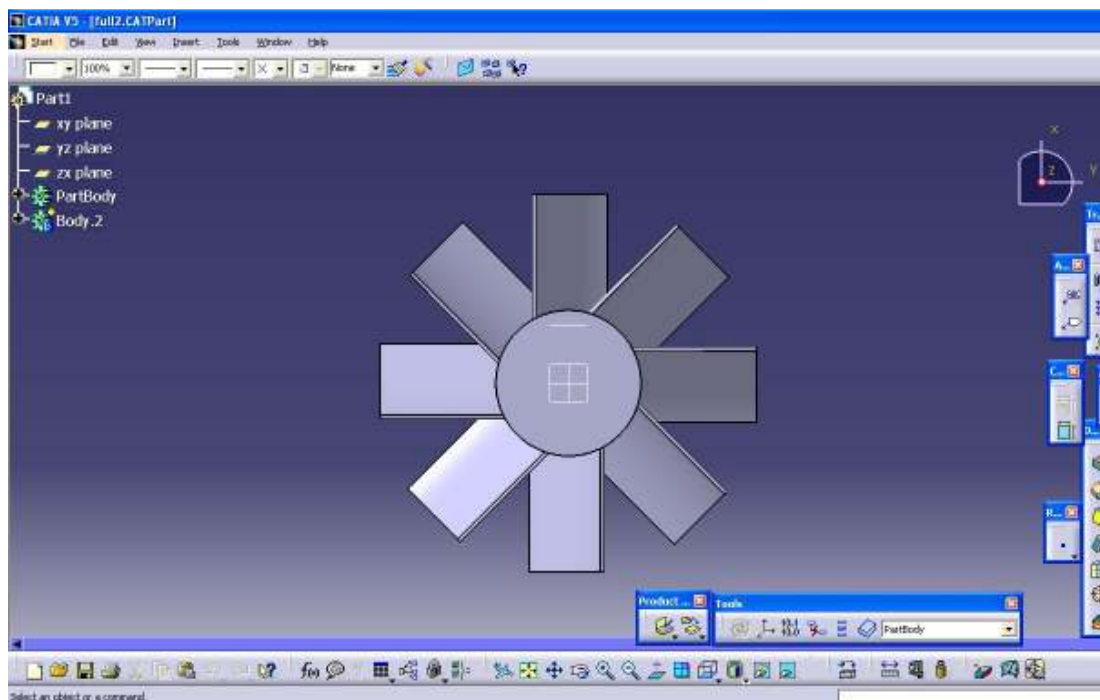
Figure 4.1: The front view of the turbine blade
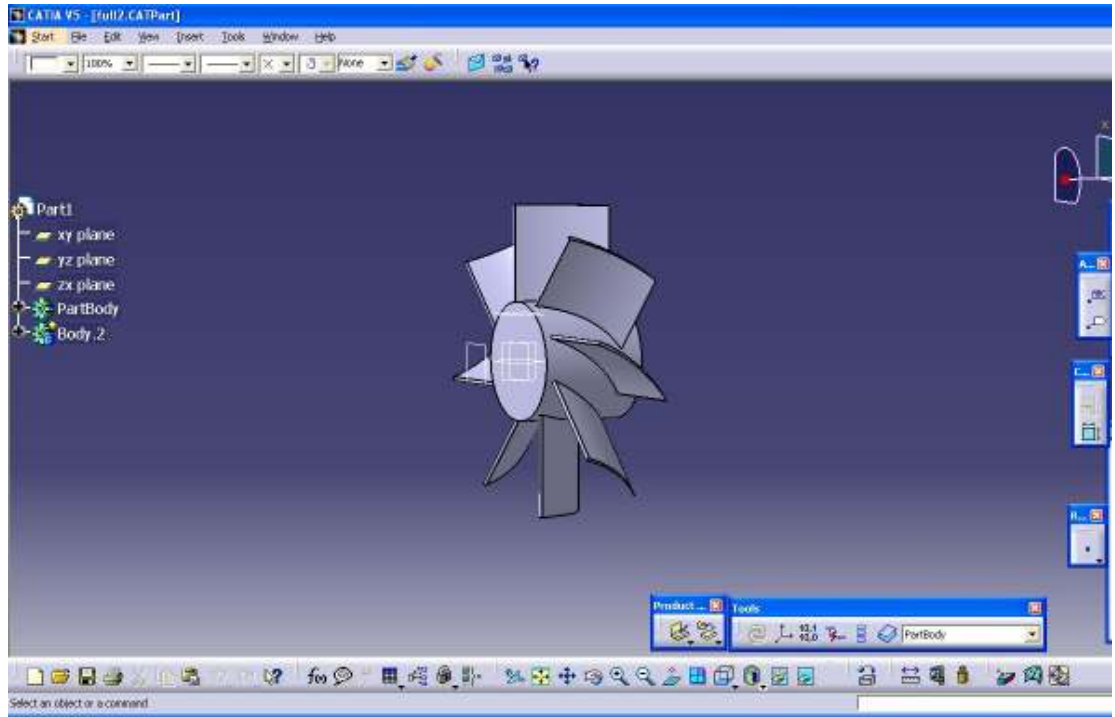
Figure 4.2: Isometric View of the Turbine Blade
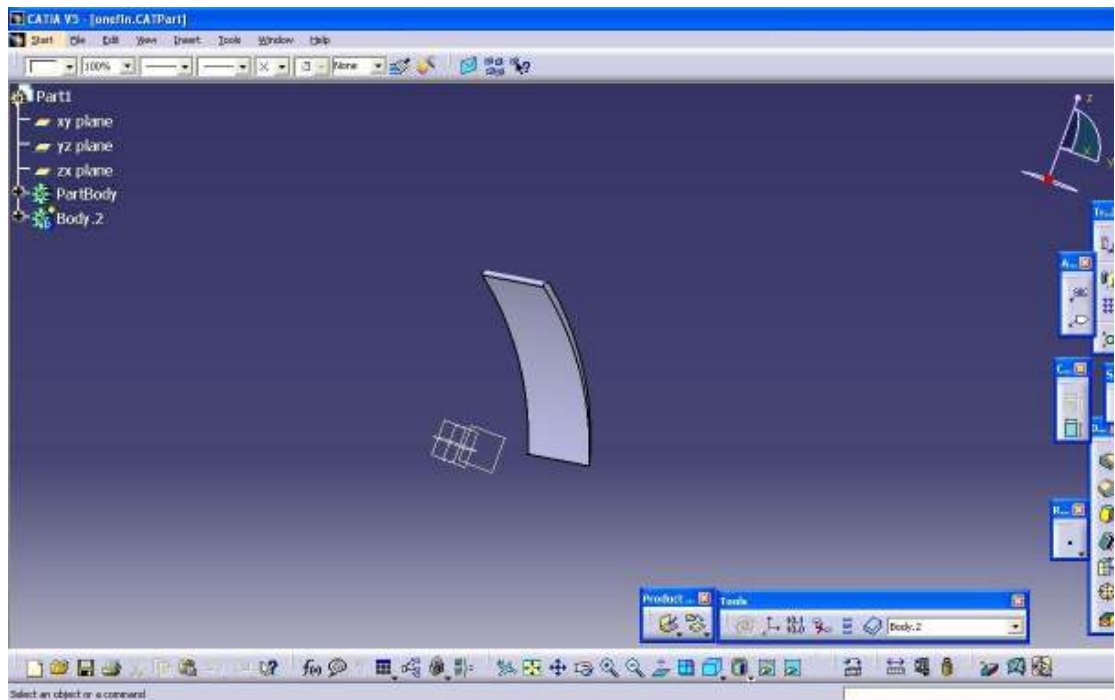
Figure 4.3: Single blade taken from the Turbine Blade
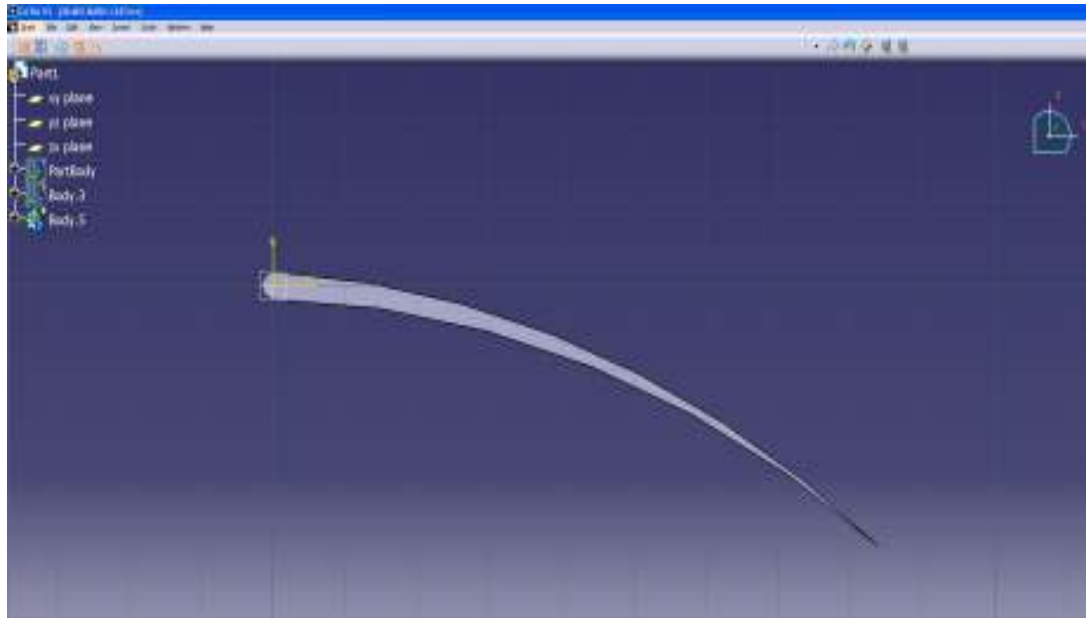
Figure 4.4: Side view of the single blade

4.1.2 Meshing of the Turbine Blade

As discussed in the methodology section 3.5, the meshing is done in ANSYS. The element chosen for the meshing is Solid 10Node187 and the element sizing is set at 2mm. Figure 4.5 shows the meshing of the turbine blade with having constraints. The area where the constraints were applied represents the area where the blade connects with the rotor blade.
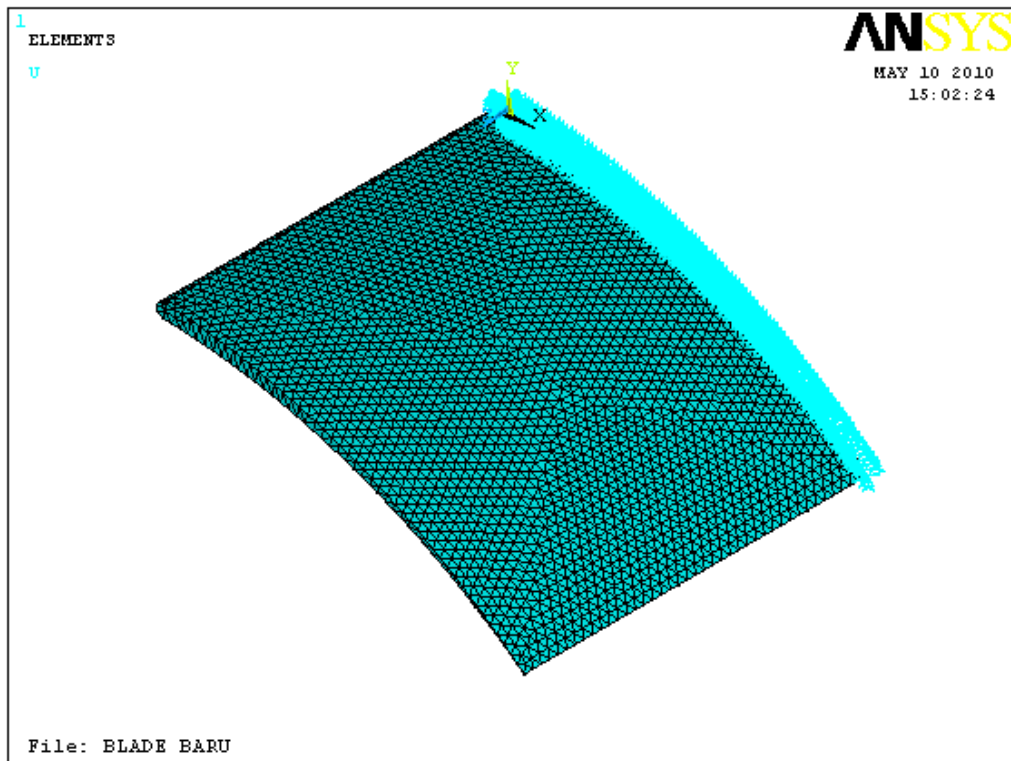
Figure 4.5 Isometric View of the Turbine Blade Meshing

4.1.3 Stress Analysis with a Uniformly Distributed Load

For the first stage of the stress analysis, the load which is applied is assumed to be the same throughout the bottom and the top surface of the turbine blade. The load which was applied on the turbine blade is pressure. Figure 4.6 shows the where the pressure was applied.
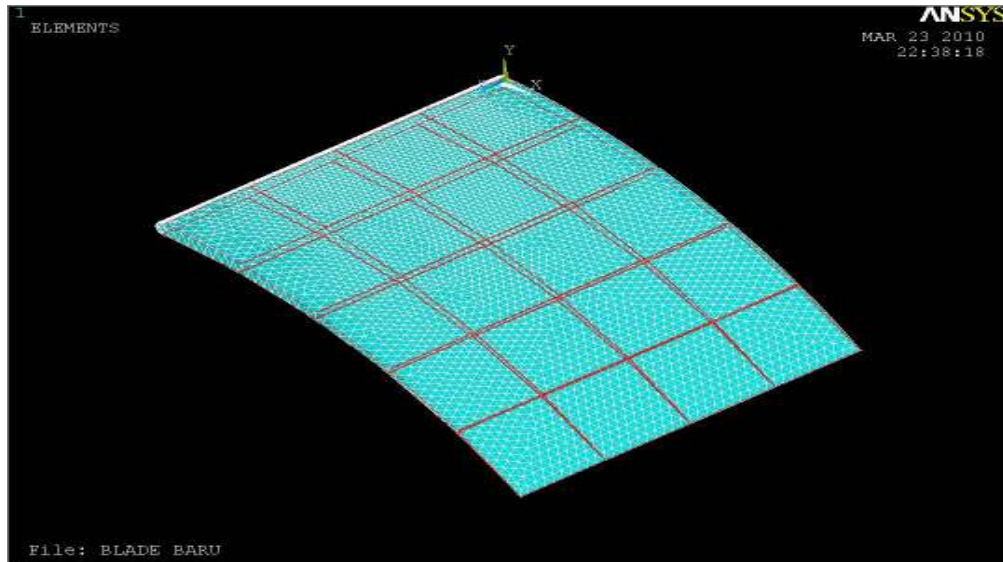
Figure 4.6: Pressure load being applied on the Turbine Blade Meshing
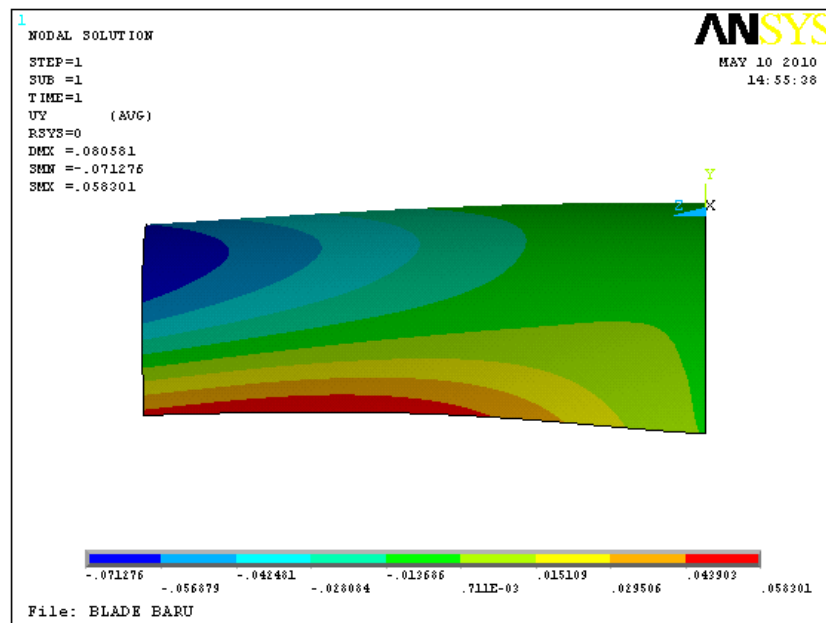
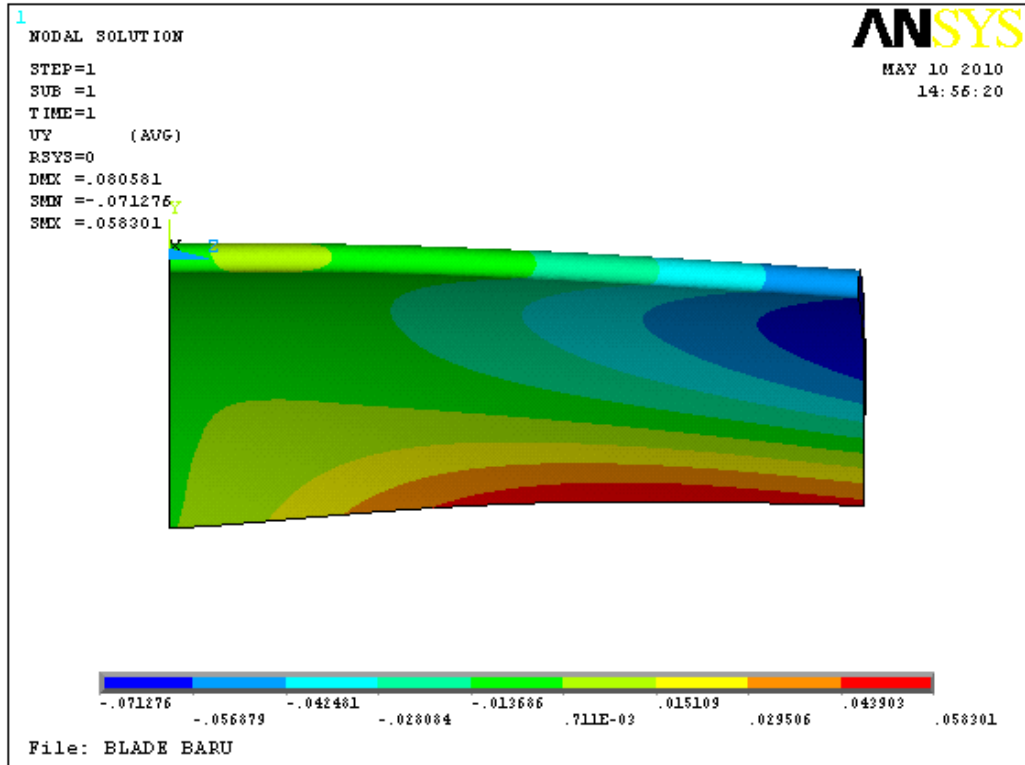
Figure 4.7: Displacement on the turbine blade after load has been applied

Figure 4.8: Front view of the displacement of the turbine blade
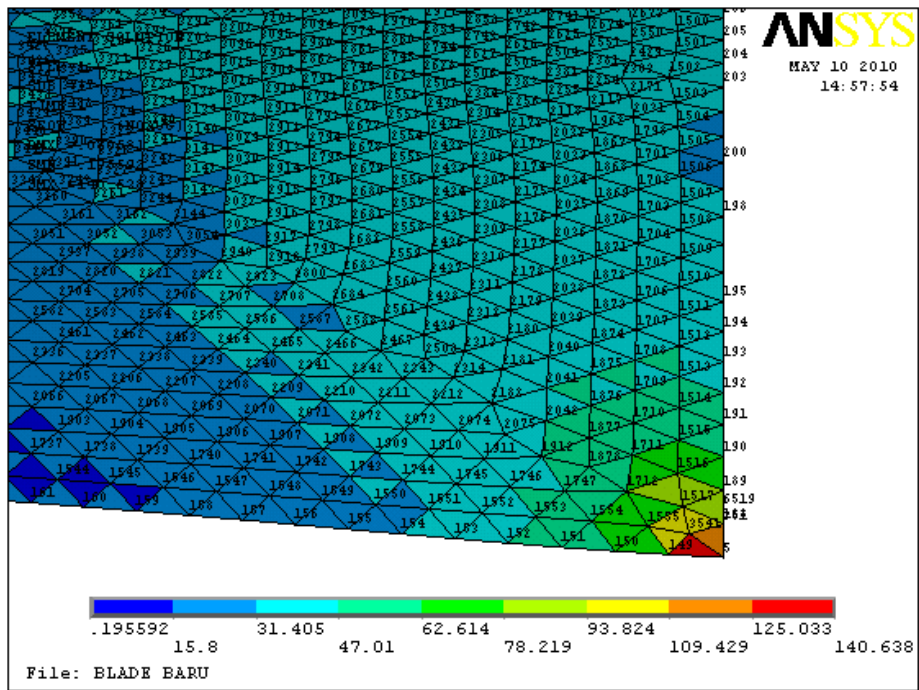
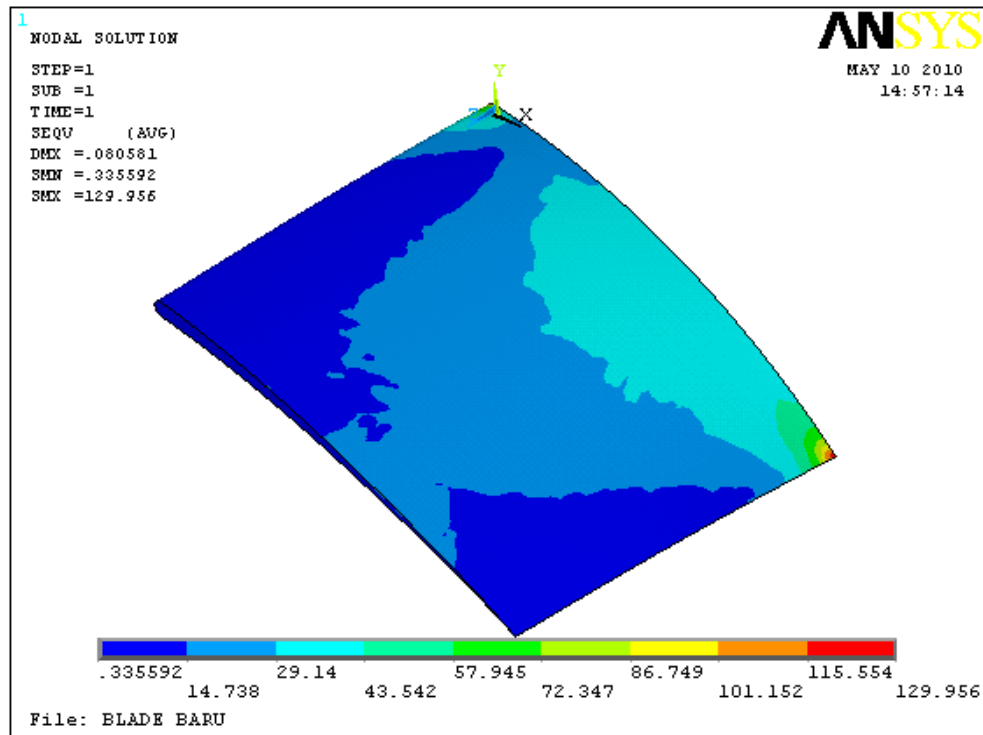Figure 4.9: Nodes Numbering on the Turbine Blade

Figure 4.10: Von Mises Stress acting towards the turbine blades

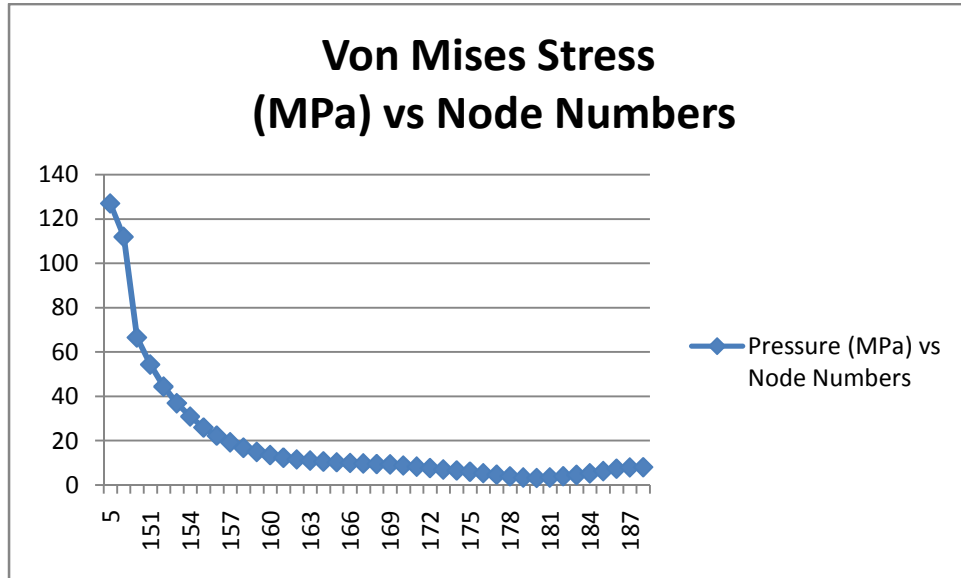Figure 4.11: List of Von Mises Stress acting on each node

Figure 4.12: Graph of the Von Mises stress values acting towards the nodes

4.1.4 Stress Analysis with Actual Pressure Distribution

For the second stage of the stress analysis, an actual pressure distribution on the turbine blade had been done. As discussed in the methodology section, it is assumed that the turbine blades have the same pressure distribution with the NACA 4415 airfoil.
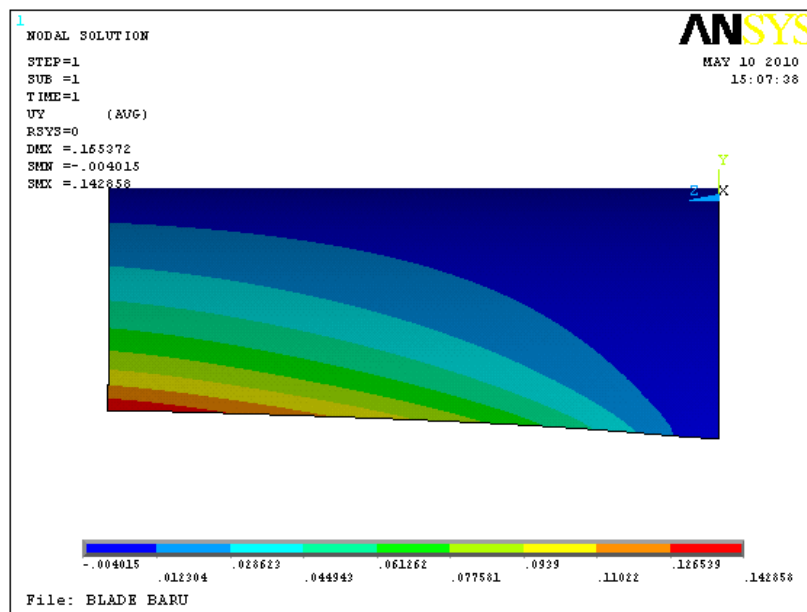
Figure 4.13: Displacement on the turbine blade after load has been applied

31
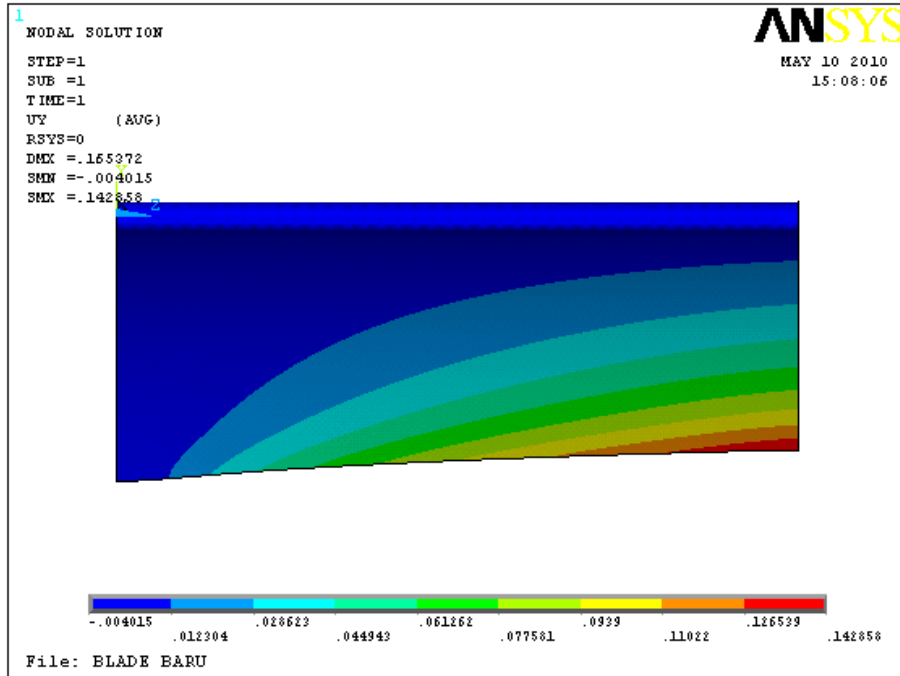
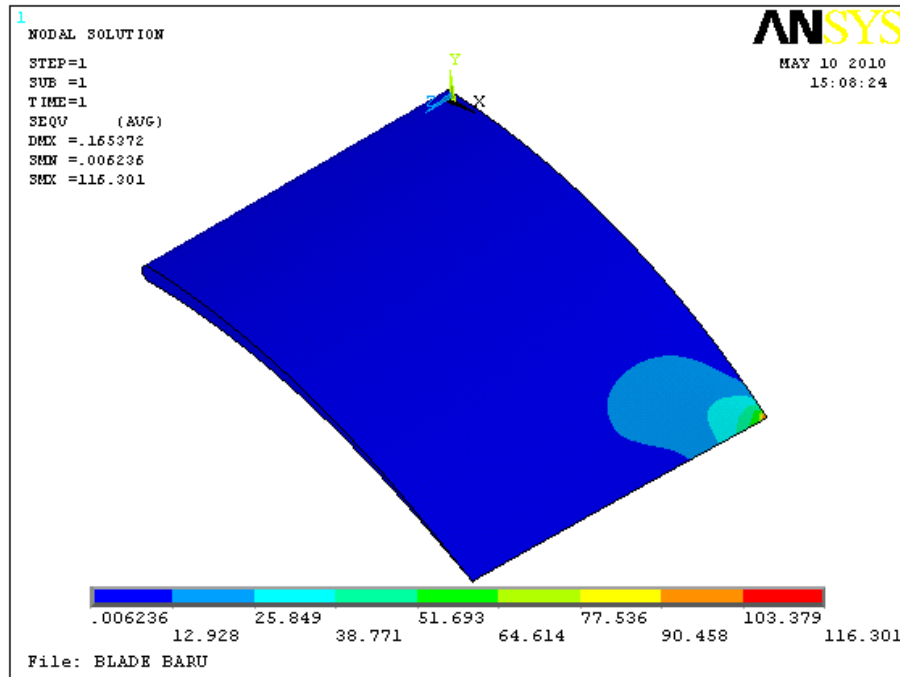Figure 4.14 Displacement on the turbine blade from the front view

Figure 4.15 Von Mises Stress acting towards the turbine blades
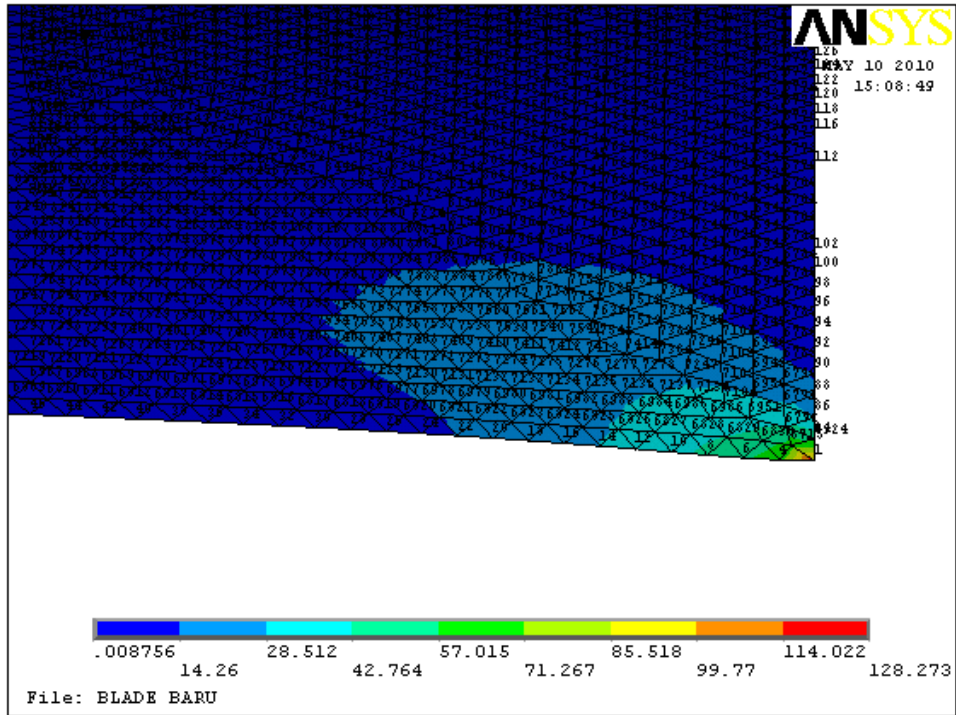
Figure 4.16: Nodes Numbering on the Turbine Blade

Figure 4.17: List of Von Mises Stress acting on each node
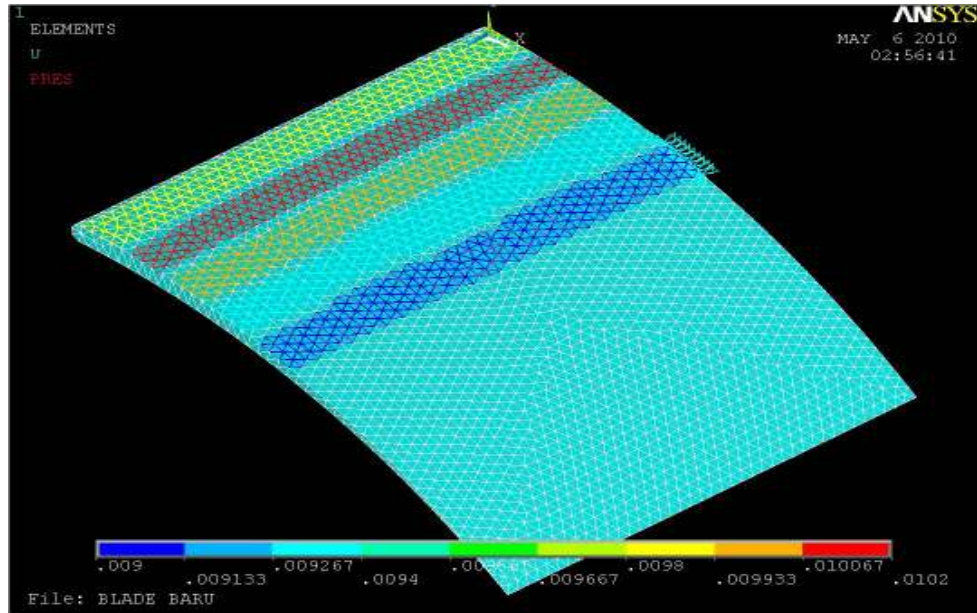
Figure 4.18: Example of different pressures applied on the Turbine Blade
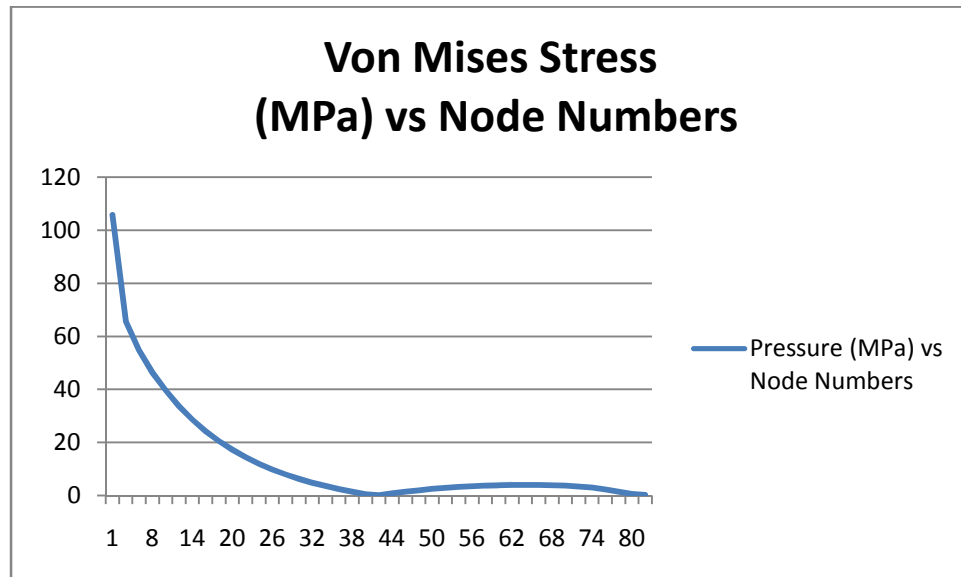
Figure 4.19: Graph of the Von Mises stress values acting towards the nodes

4.1.5 Manual Calculation

Two plane bending stress:

$$\sigma_x = -\frac{M_z}{I_z}\,y + \frac{M_y}{I_y}\,z \qquad (11)$$

F$_2$

F$_1$
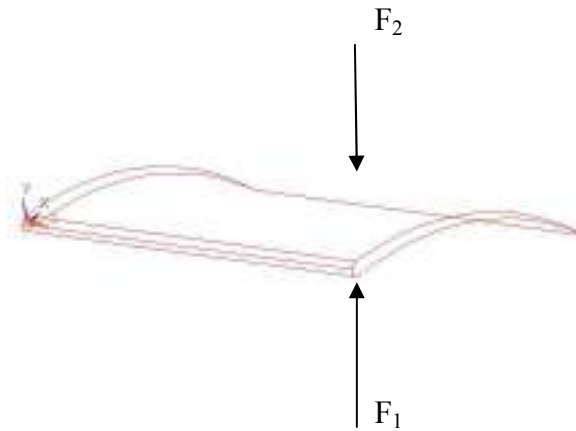
Area = Chord length X Width   (8)

$$= 0.0894 \times 0.08 \text{ m}$$

$$= 0.0072 \text{m}$$

Pressure = Force/Area   (12)

$$F_1 = 8026500 \text{Pa X } 0.0072 \text{m}$$

$$= 57791 \text{N}$$

$$= 57.79 \text{kN}$$

$$F_2 = 8000000 \text{Pa X } 0.0072 \text{m}$$

$$= 57600 \text{N}$$

$$= 57.6 \text{ kN}$$

Assume that it is rectangular,
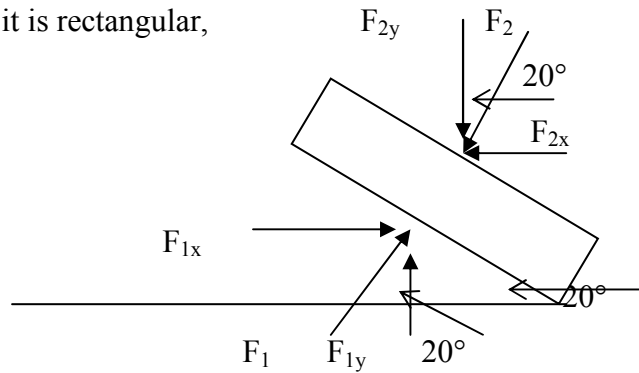
$F_{1y} = 57.79kN \cos 20°$

$\quad = 54.3$ kN

$F_{1x} = 57.79kN \sin 20°$

$\quad = 19.77$ kN

$F_{2y} = 57.6kN \cos 20°$

$\quad = 54.13$ kN

$F_{2x} = 57.6kN \sin 20°$

$\quad = 19.7$ kN

Moment calculation
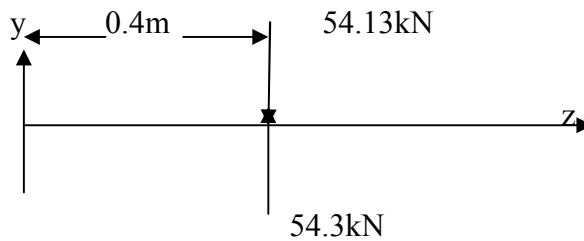
$M_x = (54.3kN \times 0.4m) - (54.13kN \times 0.4m)$

$\quad = 0.068$ kN.m
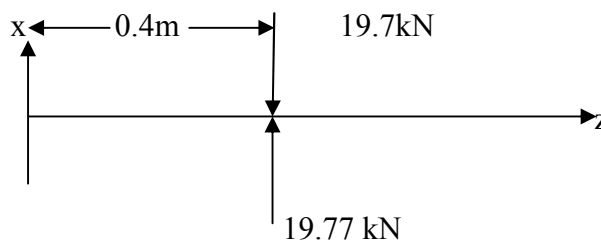
$M_y = (19.77kN \times 0.4m) - (19.7kN \times 0.4m)$

$\quad = 0.028$ kN.m

36
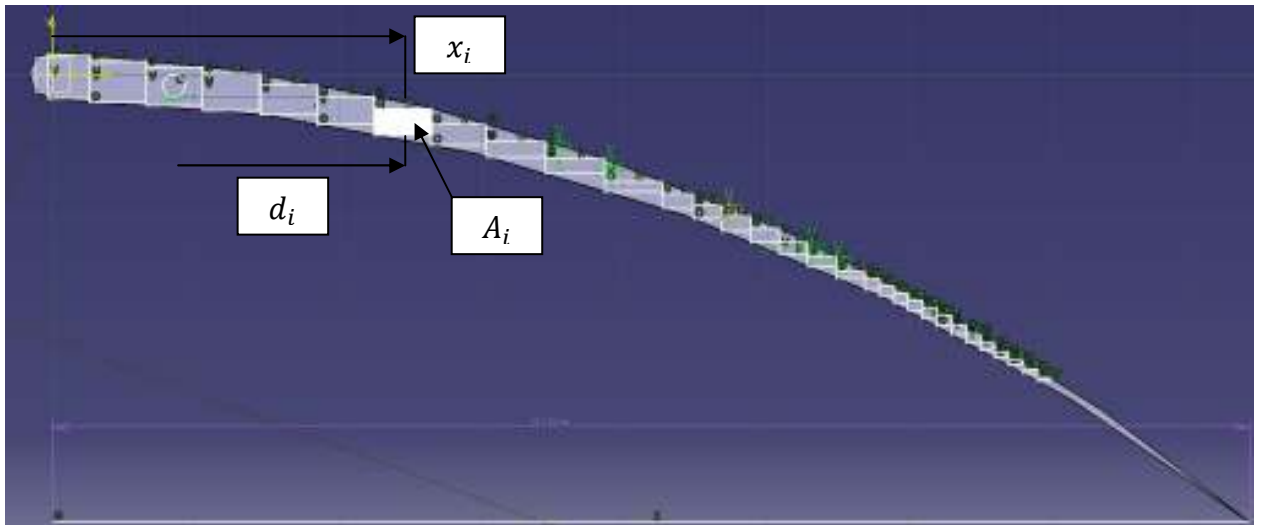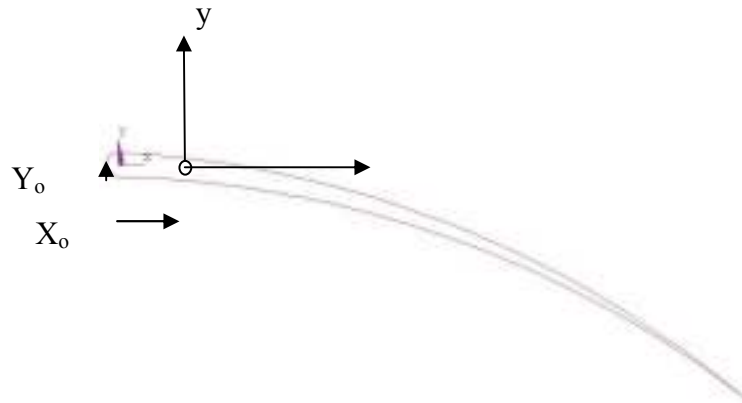
Figure 4.20: Small rectangulars being divided on the blade

To calculate the area moment of Inertia, the blades will be needed to be divided into small rectangulars. Figure 4.20 shows the blades after it has been divided into small rectangulars. Each of the rectangular areas are to be calculated. The white box in Figure 4.20 shows the current rectangular which is to be calculated. However the centroid of the airfoil is to be determined.This is because the value of d_i is needed to calculate the area moment of inertia. The distance of the centroid from the origin can be detemined using this formula:

$$x_o = \frac{\Sigma\, x_i A_i}{\Sigma\, A_i} \qquad (13)$$

Where x_o = distance of the centroid from the origin in the x direction

x_i = distance from the origin to the current calculated area

A_i = The current calculated area

Area Moment of Inertia:

$$I_x = \Sigma\, \left(\frac{bh^3}{12} + A_i d_i^2\right) \qquad (14)$$

The calculations were done in Microsoft Excel 2007 since there are many rectangulars which were divided.

Table 4.1: Data to calculate the centroid

Number	Width (m)	Height (m)	$A_i\ (m^2)$	x_i	x_i X A_i
1	0.002905	0.002973	8.63657E-06	0.001386	1.19703E-08
2	0.003943	0.002866	1.13006E-05	0.004291	4.8491E-08
3	0.003933	0.002718	1.06899E-05	0.008233	8.80099E-08
4	0.004	0.002526	0.000010104	0.012177	1.23036E-07
5	0.004	0.002018	0.000008072	0.016177	1.30581E-07
6	0.003975	0.001964	7.8069E-06	0.020213	1.57801E-07
7	0.003994	0.001833	7.321E-06	0.024188	1.7708E-07
8	0.003796	0.001412	5.35995E-06	0.028182	1.51054E-07
9	0.004191	0.001078	4.5179E-06	0.031977	1.44469E-07
10	0.00414	0.000998	4.13172E-06	0.036182	1.49494E-07
11	0.004006	0.00069	2.76414E-06	0.040308	1.11417E-07
12	0.002148	0.00101	2.16948E-06	0.044314	9.61383E-08
13	0.002	0.000897	0.000001794	0.046503	8.34264E-08
14	0.002006	0.000987	1.97992E-06	0.048503	9.60322E-08
15	0.001998	0.000999	1.996E-06	0.050509	1.00816E-07
16	0.002	0.000812	0.000001624	0.052507	8.52714E-08
17	0.002	0.000625	0.00000125	0.054503	6.81288E-08
18	0.002006	0.000432	8.66592E-07	0.056518	4.8978E-08
19	0.001	0.000765	0.000000765	0.058522	4.47693E-08
20	0.001005	0.000689	6.92445E-07	0.05953	4.12213E-08
21	0.001005	0.000678	6.8139E-07	0.060535	4.12479E-08
22	0.000999	0.000724	7.23276E-07	0.06154	4.45104E-08
23	0.001	0.000789	0.000000789	0.062539	4.93433E-08
24	0.001008	0.000742	7.47936E-07	0.063543	4.75261E-08
25	0.001052	0.000631	6.63812E-07	0.064551	4.28497E-08
26	0.001025	0.000561	5.75025E-07	0.065603	3.77234E-08
27	0.000994	0.000473	4.70162E-07	0.066602	3.13137E-08
28	0.000985	0.000415	4.08775E-07	0.067595	2.76311E-08
29	0.000988	0.00033	3.2604E-07	0.06858	2.23598E-08
30	0.001	0.000256	0.000000256	0.069568	1.78094E-08
31	0.001	0.000169	0.000000169	0.070537	1.19208E-08
			9.96526E-05		2.33242E-06

$$x_o = \frac{2.332\ X\ 10^{-6}}{9.965\ X\ 10^{-5}} \qquad (13)$$

$$x_o = 0.025\text{m}$$

Table 4.2 : Data to calculate the Area Moment of Inertia

Number	d_i	d_i^2	$A_i d_i^2$	$\dfrac{bh^3}{12}$	$\dfrac{bh^3}{12} + A_i d_i^2$
1	0.023614	0.0005576	4.81593E-09	2.68606E-10	5.08454E-09
2	0.020709	0.0004289	4.84642E-09	2.68606E-10	5.11503E-09
3	0.016767	0.0002811	3.00527E-09	2.68606E-10	3.27388E-09
4	0.012823	0.0001644	1.66139E-09	2.68606E-10	1.93E-09
5	0.008823	7.785E-05	6.28367E-10	2.68606E-10	8.96973E-10
6	0.004787	2.292E-05	1.78898E-10	2.68606E-10	4.47504E-10
7	0.000812	6.593E-07	4.82706E-12	2.68606E-10	2.73433E-10
8	0.003182	1.013E-05	5.42702E-11	2.68606E-10	3.22876E-10
9	0.006977	4.868E-05	2.19925E-10	2.68606E-10	4.8853E-10
10	0.011182	0.000125	5.16618E-10	2.68606E-10	7.85224E-10
11	0.015308	0.0002343	6.47734E-10	2.68606E-10	9.1634E-10
12	0.019314	0.000373	8.09282E-10	2.68606E-10	1.07789E-09
13	0.021503	0.0004624	8.29508E-10	2.68606E-10	1.09811E-09
14	0.023503	0.0005524	1.09369E-09	2.68606E-10	1.3623E-09
15	0.025509	0.0006507	1.29882E-09	2.68606E-10	1.56742E-09
16	0.027507	0.0007566	1.22878E-09	2.68606E-10	1.49738E-09
17	0.029503	0.0008704	1.08803E-09	2.68606E-10	1.35664E-09
18	0.031518	0.0009934	8.60859E-10	2.68606E-10	1.12946E-09
19	0.033522	0.0011237	8.59649E-10	2.68606E-10	1.12825E-09
20	0.03453	0.0011923	8.25617E-10	2.68606E-10	1.09422E-09
21	0.035535	0.0012627	8.60416E-10	2.68606E-10	1.12902E-09
22	0.03654	0.0013352	9.65698E-10	2.68606E-10	1.2343E-09
23	0.037539	0.0014092	1.11184E-09	2.68606E-10	1.38045E-09
24	0.038543	0.0014856	1.11111E-09	2.68606E-10	1.37971E-09
25	0.039551	0.0015643	1.03839E-09	2.68606E-10	1.30699E-09
26	0.040603	0.0016486	9.47988E-10	2.68606E-10	1.21659E-09
27	0.041602	0.0017307	8.13722E-10	2.68606E-10	1.08233E-09
28	0.042595	0.0018143	7.41654E-10	2.68606E-10	1.01026E-09
29	0.04358	0.0018992	6.19221E-10	2.68606E-10	8.87826E-10
30	0.044568	0.0019863	5.08494E-10	2.68606E-10	7.771E-10
31	0.045537	0.0020736	3.50442E-10	2.68606E-10	6.19047E-10
					4.28696E-08

$$I_x = 4.29 \times 10^{-8} \; m^4$$

$$I_y = \frac{bh^3}{12}$$

$$I_y = \frac{0.0033 \, X \, 0.0895^3}{12}$$

$$I_y = 1.97 \, X \, 10^{-7}$$

$$\sigma_z = -\frac{M_x}{I_x}y + \frac{M_y}{I_y}x$$

$$\sigma_z = -\left(\frac{0.068}{4.29 \, X \, 10^{-8}}\right)(-0.031) + \left(\frac{0.028}{1.97 \, X \, 10^{-7}}\right)(0.0838)$$

$$\sigma_z = 49137.53 + 11910.66$$

$$\sigma_z = 61048.19 \, \text{kPa}$$

$$\sigma_z = 61.05 \, \text{MPa}$$

4.2. DISCUSSION

4.2.1 The Design of the Turbine Blade

The rotor blade design was based on the Brooks Parity turbine flowmeter from Fisher-Rosemount Petroleum. The turbine meter is a 12 inch model. Two designs were made which are the rotor blade and the single turbine meter blade. For the stress analysis, only the single turbine blade design will be used. Even though the design was based on the Brooks Parity turbine flowmeter, the design was not done using the actual specification of the flowmeter. This is due to the patent issue and the actual specification of the turbine blade was not available. The rotor blade was designed based on the shape of the original turbine flowmeter. The turbine blade has an airfoil design. The blade is designed

is such way that the angle is 20 degrees of the flow of water. This is because a standard turbine flowmeter operates between 20 to 40 degrees of angle.

4.2.2 Stress Analysis with a Uniformly Distributed Load

The first stage of the stress analysis which is the stress analysis with a uniformly distributed load was conducted in order to see a simple view on how stress acts towards the turbine blade. The pressure load which is acting on the top surface of the blade is 8000kPa which is the water injection pressure in the pipeline. For the pressure which is acting on the bottom surface of the turbine blade, the value of the pressure is represented by:

$$\text{Total Bottom Surface Pressure} = P + \frac{L}{A}$$

(7)

With P = Water Pressure = 8000kPa

L = Lift Force

A = Area = Chord Length X Width

Figure 4.6 shows the turbine blade with the pressure being applied on the top and the bottom surface. The red lines situated on the surface represent the pressure and it shows the value of the pressure is the same throughout the surface.

Figure 4.10 shows the Von Mises stress which is acting towards the turbine blades. From ANSYS, the maximum stress which is acting on the nodes is 129.96MPa. As shown in Figure 4.9 and 4.10, high stress occurs near where the constraints are applied. It is expected for the stress to occur along that region. However, the highest stress only occurs in the region where the turbine blade is at the thinnest thickness. For 430 Stainless Steel, the yield strength is around 430 MPa. If the stress which occurs on the turbine blade is higher than the yield strength, permanent deformation will occur. However in this case, the maximum Von Mises stress is below the yield strength of the material.

42

Figure 4.7 and 4.8 shows the deflection of the turbine blade. From those two figures, it is shown that the turbine blade goes through a little deformation when the loads are acting towards the turbine blades. The maximum displacement for the simulation is 0.071mm. From figure 4.8, it can be seen that the turbine blades are bent downwards on the right side of the blade and from figure 4.7, it can be seen that the left side of the turbine blade are bent upwards with a deflection of 0.058mm. Even though the turbine blades have a slight deformation when the loads are applied, it is expected that the turbine blades will return to its original form since the Von Mises stress calculated from the simulation is lower than the yield strength of the material. However failure could still occur due to tear and wear since the blade tends to deform when pressure is applied to it. Figure 4.12 shows the graph of the Von Mises stress values which are acting towards the nodes. The nodes which are selected are the nodes located along the Z axis and at the thinnest part of the blade. Figure 4.9 shows an example of the nodes numbering. From the graph, it can be seen that Node number 5 has the biggest Von Mises stress value due to its location which is at the constraints. As it move along nodes on the Z axis, the value of the Von Mises stress decreases. This proves that higher stress will occur at the location where the constraints are applied.

4.2.3 Stress Analysis with Actual Pressure Distribution

The stress analysis with an actual pressure distribution is the final stage of the project. As discussed previously the pressure distribution of the turbine blade is assumed to be the same with the pressure distribution of NACA 4415 airfoil. This assumption was made to reduce the complications of finding the turbine blades actual pressure distribution. With this assumption, data calculations were also made possible since data such as lift coefficient.

From the data in Figure 3.6, the pressure distribution coefficient was calculated. With the pressure distribution coefficient, the actual pressure at the specific point of the airfoil can be calculated. The results of the calculation are shown in Table 3.3 and 3.4. The pressure applied on the turbine blade is divided to 10 different sections. This is to simulate the different values of pressure distribution which is acting on the turbine

blade. Figure 4.18 shows the pressure being applied on the turbine blade. However, in that figure only 5 sections were shown. This figure is just an example of how different pressure loads applied looks like in ANSYS. The different colours represent different pressure values. This step is repeated for the bottom surface as well.

Figure 4.13 and Figure 4.14 shows the deflection of the turbine blade when an actual pressure distribution is used. It can be seen in Figure 4.13 that the highest displacement occurs at the left side of the blade. This part of the blade also has a very thin thickness. The maximum displacement for this simulation is 0.14mm. In Figure 4.13 as well, we can see that the turbine blade is slightly bent when the pressure load is applied. However, it will return to its original shape when there is no pressure load acting towards it.

Figure 4.15 and 4.16 shows the Von Mises stress which are acting towards the turbine blade. From both of the figures, it can be seen that the maximum stress is concentrated at the thinnest part of the turbine blade where the constraints are applied. The maximum Von Mises stress which acts towards the turbine blades is 116.3MPa. This is 13.66MPa less than the stress analysis which was done with uniformly distributed pressure. This is logical since the actual pressure distribution has a lower pressure value and the value varies at different length of the turbine blades. As discussed in the previous section, the yield strength of the 430 stainless steel is around 430MPa. Since the maximum Von Mises stress is lower than the yield strength of the material, it can be concluded that the turbine meter blades will not fail under the current operating condition of the water injection pipeline. However, further studies should also be made to verify this conclusion.

From this simulation, it is found that the pattern of Von Mises stress is quite similar to the simulation using the uniformly distributed pressure. Stress occurs throughout the entire turbine blade. Most of the sections only experience a small value of stress. A value as which is as low as 0.34MPa. This is considered low if it is compared to the highest pressure. The highest pressure is located where the constraints are applied. It is also situated at the thinnest section of the blade. This is maybe due to the fact that it is

easier to bend at the thin area of the blade. Figure 4.19 shows the graph of the Von Mises stress values which are acting towards the nodes. This graph shows that the results obtained are similar to the results for the Stress Analysis with Uniformly Distributed Pressure. The nodes which are selected are the nodes located along the Z axis and at the thinnest part of the blade. Figure 4.16 shows an example of the nodes numbering. From the graph, it can be seen that Node number 1 has the biggest Von Mises stress value due to its location which is at the constraints. As it move along nodes on the Z axis, the value of the Von Mises stress decreases. This proves that higher stress will occur at the location where the constraints are applied.

4.2.4 Manual Calculations

For this project, the manual calculation is based on the two plane bending technique. The two plane bending technique states that bending usually occurs in both the xy and xz planes. Considering the cross sections with one or two planes of symmetry only, the bending stresses are given by:

$$\sigma_x = -\frac{M_z}{I_z} y + \frac{M_y}{I_y} z \qquad (11)$$

This approach was taken since this equation can be used to identify the value of the bending stress at a particular point of the object. This was useful since, the results from ANSYS can now be compared with the manual calculations. The manual calculation will calculate the bending stress at the point where the turbine blade is the thinnest and where the constraints are applied. This is because in the simulation, the highest stress is located at that particular point. This can be seen in Figure 4.15.

In the simulation in ANSYS, the highest Von Mises stress is 116.3 MPa while the manual calculation gave a result of only 61.05 MPa. This gives a big difference of 55.25 MPa. The manual calculation might have certain confines. For instance, the shape of the

turbine blade is not uniform. Thus, it is difficult to calculate the actual size of the airfoil area of the turbine blade. Another reason to this might be the approach that had been taken to calculate the stress. Maybe a different approach can be taken so that the value of stress calculated will be more accurate. Besides that, assumptions were made in both the manual calculation and the simulation. Due to this, a difference in results is possible.

CHAPTER 5

CONCLUSION AND RECOMMENDATIONS

5.1 CONCLUSION

Stress Analysis plays an important role especially in designing an object. For example, building bridges. The engineer or the architect needs to ensure the bridge can withstand a certain value of load. This is helpful to prevent the bridge from collapsing. With the aid of ANSYS, the stress acting towards an object may be obtained. The stress could also be calculated manually however in ANSYS, the user can identify where exactly the highest stress are.

From the results of this project, the objectives which was discussed in Chapter 1 is achieved. The first objective is to analyse how stress acts on the water injection turbine meter blades. With the result of this project, it is learned that stress may occur throughout the entire object. However, the highest stress would normally be at area where the constraints are applied. This can be proven from the results obtained. The highest stress would also be concentrated at the thinnest part of the object. In this project, the designs of the blade are in such way that it is an airfoil design. Due to this, the thickness of the blades, were thinner towards at the right end of the blade. The second objective is to study whether the high pressure difference is the cause of the bent turbine blades. At the initial stage of the project, it was believed that the blades are bent due to the high pressure difference during water injection back-on-line. The turbine blades were experiencing a pressure change from 0 to 8000kPa. However, after doing the stress analysis on the turbine blades, it was found that the blade's Von Mises stress were lower than the yield strength of the materials used to build the turbine blades. From

the results of the stress analysis, it was found that the turbine blade was having displacement when the pressure load was applied to it. However, since the Von Mises stresses on the blade were lesser than the yield strength of the material, it is expected the turbine blade will return to its original shape when no pressure load is being applied to it. Due to the displacement of the blades, it is expected that the turbine blade could still fail due to tear and wear. Different and other analysis are required the causes of the bent turbine blades.

This report describes the stages of the analysis development. It describes the designing stage of the turbine blades, the initial stage of the stress analysis as well as the final stage of the stress analysis which the actual pressure distribution was used. In this case, the actual pressure distribution means the NACA 4415 airfoil pressure distribution since it was assumed that the turbine blades have the same design as the NACA 4415 airfoil. This is basically to decrease the complexity of this project.

With this project, it is hoped that a better design of the turbine blades could be created in the future. Turbine flowmeters are widely used in the oil and gas industry today. However, currently manufacturers states that one type of flowmeter can be used for many types of liquids. For example, the manufacturer states that one of its specific turbine flowmeter could be used for oil as well as water injection. Sometimes, the turbine flowmeter could work wonderfully for oil usage but it may not be the same for water injection. These two liquids operate at different pressures and velocities. It would be great if the manufacturer could build a turbine flowmeter specifically for the usage of water injection so that it can withstand the operating conditions of the water injection pipelines.

5.2 RECOMMENDATIONS

For this project, some improvements could be made to give a better and more accurate results. The improvements are listed as below:

1) Design the turbine blades to the exact specification and dimensions
   - In this project, the design was based from the Brooks Parity turbine flowmeter from Fisher-Rosemount Petroleum. The design was created in such way that it has a similar design. This was because it was difficult to get the original specifications from the manufacturer due to the patent of the turbine flowmeter.
2) Run an analysis which determines the actual coefficient of pressure distribution for the turbine blade.
   - As discussed previously, the turbine blades were assumed to have the same pressure distribution with NACA 4415 airfoil. This was done to reduce the complexity of the project and the data of NACA 4415 airfoil are easily obtained.
3) To study the actual cause of the bent turbine blades.
   - In this project, only the static analysis was done because the main objective of the project is to study whether the high pressure difference during the water injection back on line is the cause of the bent turbine blades. This project mainly focus of the stress caused by the water injection when it first touches the turbine blades. It does not study the stresses when the rotor blades are rotating. Even though it was found that the the pressure difference during water injection back on line is not the cause of the bent turbine blades, the cause of it is still not identified. Other studies such as dynamic analysis could identify this problem.
4) To do the simulation at different blade angles
   - The blade angle that was used in this project is 20° angle. This angle was chosen since the manufacturers used 20 to 40° angle for their blade angles in the turbine flowmeter. Studies on effects of different blade angles can identify the angle which can generate least stress on the turbine blades.

5) To use other materials as well for the simulation

- In this project, only one material was used for the simulation which is the 430 Stainless Steel. There a lot of other materials which are used to create a turbine blade. Therefore, a study of the types of material could also be helpful.

REFERENCES

1. Sukhvinder Kaur Bhatti, Shymala Kumari, M L Neepali, C Kedarinath and DR. I N Niranjan Kumar (2006), *Transient State Stress Analysis on an Axial Flow Gas Turbine Blades and Disk Using Finite Element Procedure*.

2. Turbine FlowmetersPart 1: Details of the Basic Axial Turbine Flowmeter. Available at: http://www.sensorsmag.com/sensors/flow/turbine-flowmeterspart-1-details-basic-axial-turbine-flowmet-843 (1 October 1999)

3. "PT" Liquid Turbine Meter Brochure (1999)

4. Turbine Flowmeters for Liquid Measurement. Available at :
   <http://www.flowmeterdirectory.com/flowmeter_artc/flowmeter_artc_02011701.html> (January 2002)

5. Kid Wind Project. *Advanced Wind Turbine Blade Design*

6. Pilkey, Walter D, (2005) John Wiley & Sons. *Formulas for Stress, Strain, and Structural Matrices (2nd Edition)*

7. Turbine Flowmeters. Available at:
   http://www.sensors-research.com/articles/turbines.htm

8. Stainless Steel – Grade 430. Available at:
   http://www.azom.com/Details.asp?ArticleID=996

9. Budynas, Richard G. And Nisbett, J. Keith (2008) *Shigley's Mechanical Engineering Design*. McGraw Hill

10. Hibbeler, R. C. (2005) *Mechanics of Materials.* Pearson Prentice Hall

11. R L Reuss, M J Hoffman, G M Gregorek (December 1995), *Effects of Surface Roughness and Vortex Generators on the NACA 4415 airfoil.*

12. NACA 4415 Airfoil Calculation.
    Available at http://www.symscape.com/node/293

13. Daniel Parity Turbine Meter Sizes 3-16 inch Design Specification
    Available at ://www.daniel.com

14. Backman, D. And Greene, R. J. (2008) *Gas Turbine Blade Stress Analysis and Mode Shape Determination using Thermoelastic Methods*

15. One Design Airfoil Analysis
    Available at http: ://www.eaa1000.av.org/technic1/onedesaf/1desaf.htm

APPENDIX